



The Henryk Niewodniczański
Institute of Nuclear Physics
Polish Academy of Sciences



Przejście Verweya w magnetycie - dynamika sieci i fluktuacje krytyczne

Przemysław Piekarczyk

*Zakład Komputerowych Badań Materiałów
Instytut Fizyki Jądrowej PAN*



Collaboration

K. Parlinski

Institute of Nuclear Physics, Polish Academy of Sciences, Kraków

A. M. Oleś

Institute of Physics, Jagiellonian University, Kraków

**A. Kozłowski, T. Kołodziej, W. Tabiś, Z. Kąkol, A. Tarnawski, M. Zając,
B. Handke, J. Przewoźnik, T. Ślęzak, J. Korecki**
AGH University of Science and Technology, Kraków

D. Legut

IT4Innovations, National Supercomputing Center, Ostrava

A. Bosak, M. Krisch, A. I. Chumakov

The European Synchrotron, ESRF, Grenoble

M. Hoesch

Diamond Light Source, Harwell

S. Borroni, A. Mann, F. Carbone

École Polytechnique Fédérale de Lausanne, Lousanne

J. Lorenzana

University of Rome “La Sapienza”, Rome

E. Baldini, C. A. Belvin, N. Gedik

Massachusetts Institute of Technology, Cambridge, USA

Magnetic susceptibility

Die anfängliche Suszeptibilität von Eisen und Magnetit in Abhängigkeit von der Temperatur

VON DER
EIDGENÖSSISCHEN TECHNISCHEN HOCHSCHULE
IN ZÜRICH

ZUR ERLANGUNG DER WÜRDE EINES
DOKTORS DER TECHNISCHEN WISSENSCHAFTEN
GENEHMIGTE PROMOTIONSARBEIT

VORGELEGT VON
KARL RENGER
DIPL. MASCH.-ING.
AUS BÖHM.-KAMNITZ (ÖSTERREICH)

REFERENT:
HERR PROF. DR P. WEISS
KORREFERENT:
HERR PROF. DR A. EINSTEIN

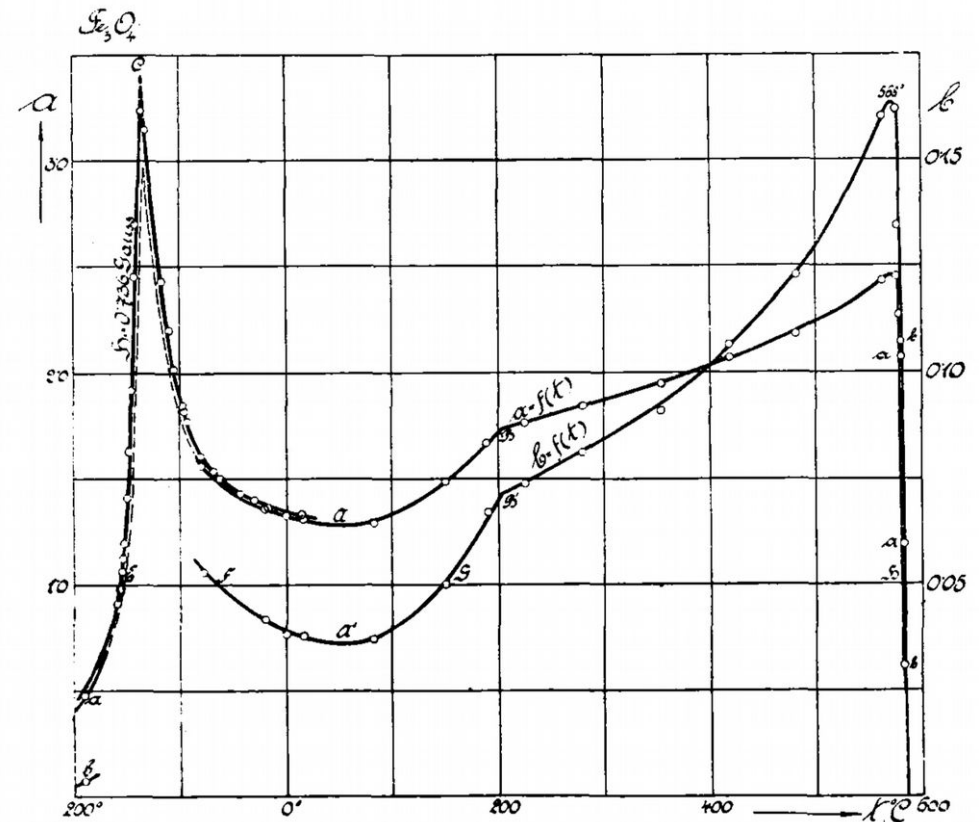
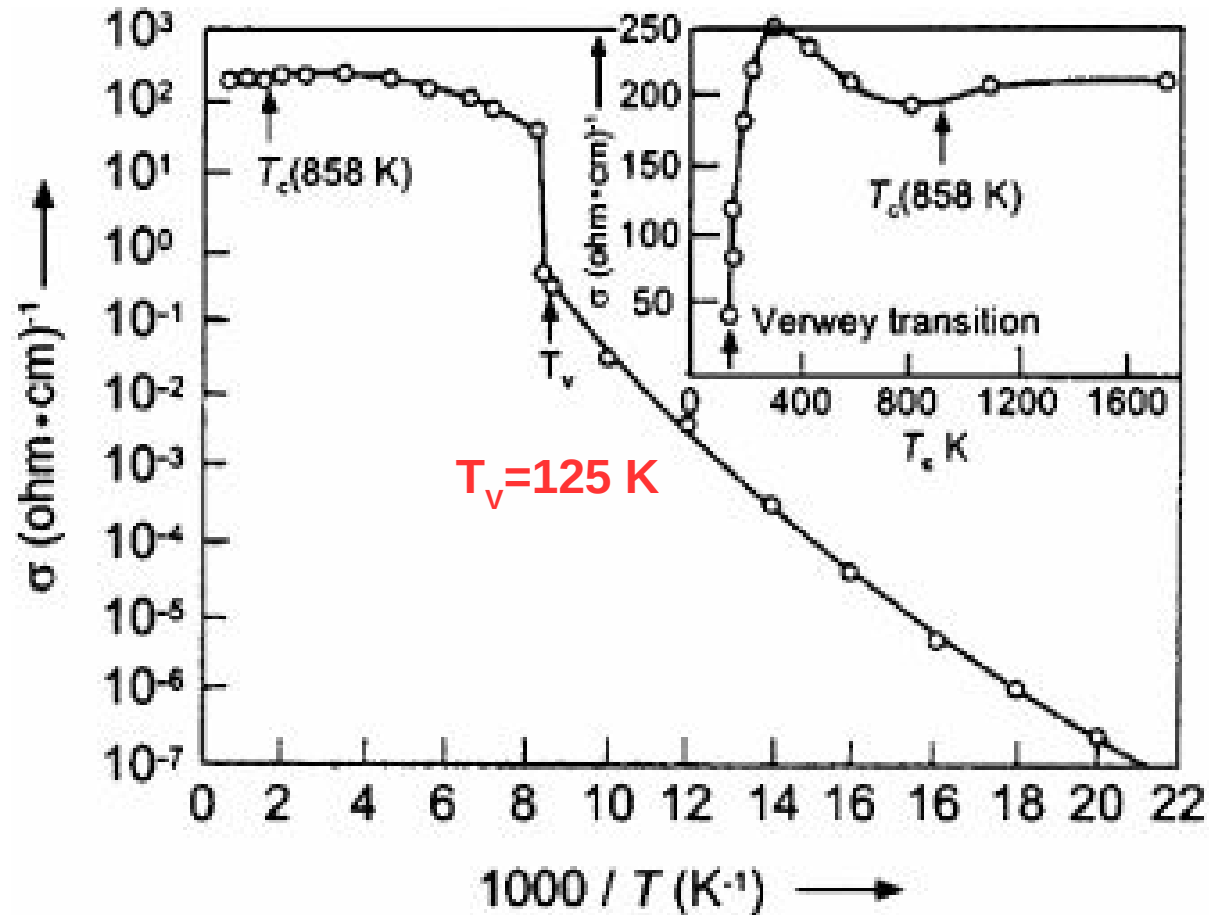


Fig. 14

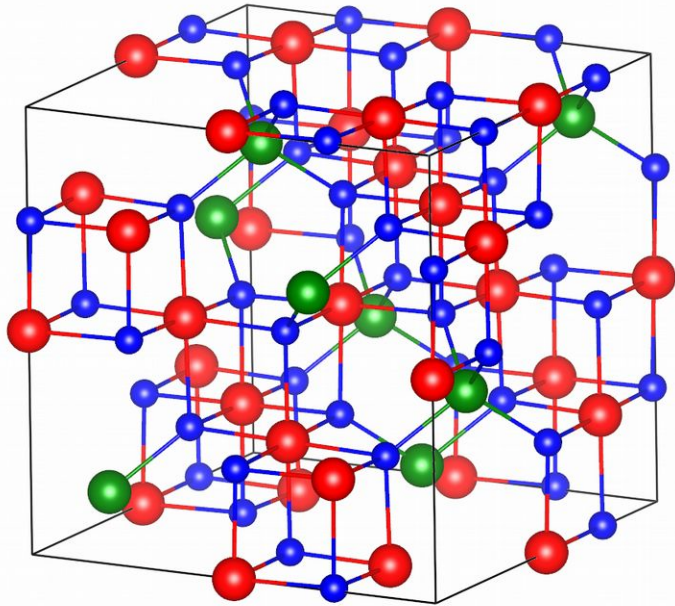
Verwey transition in magnetite Fe_3O_4

E. J. W. Verwey, Nature 144, 327 (1939)

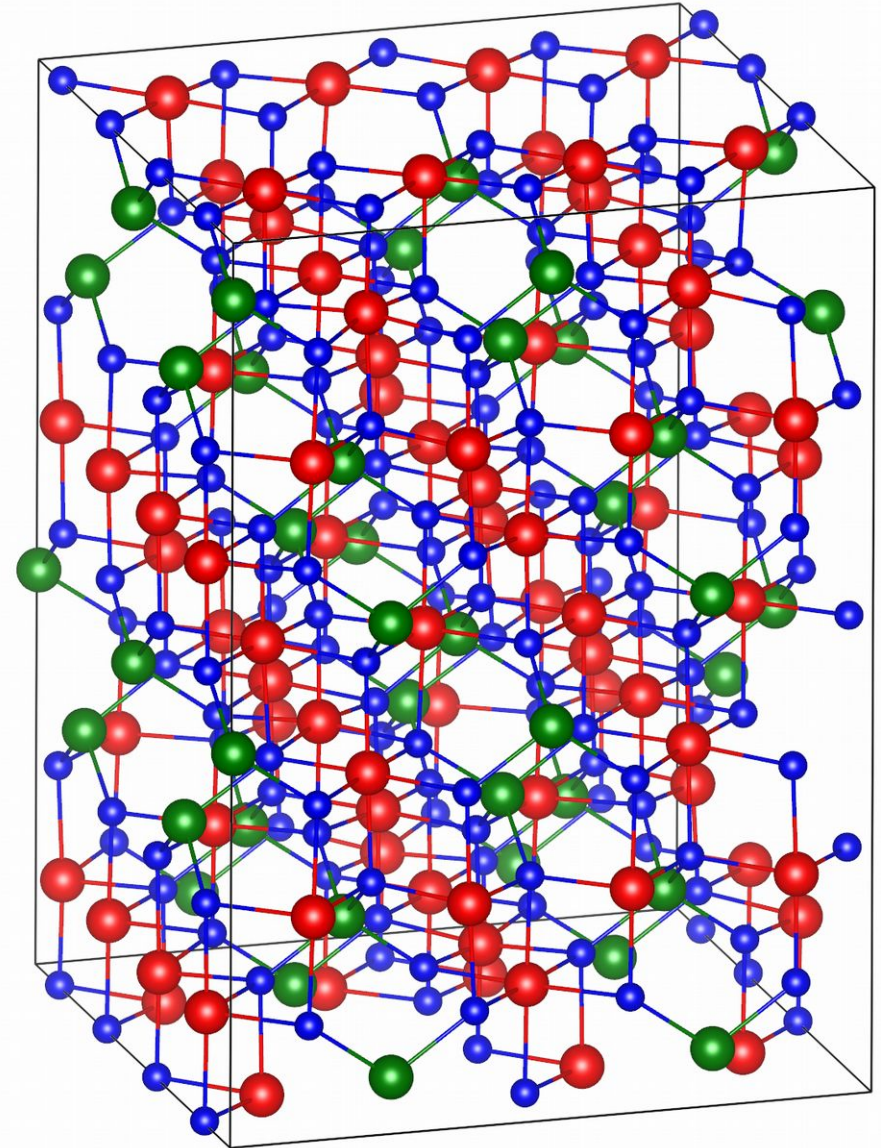


Structural phase transition

Fd-3m $T > T_v = 125$ K

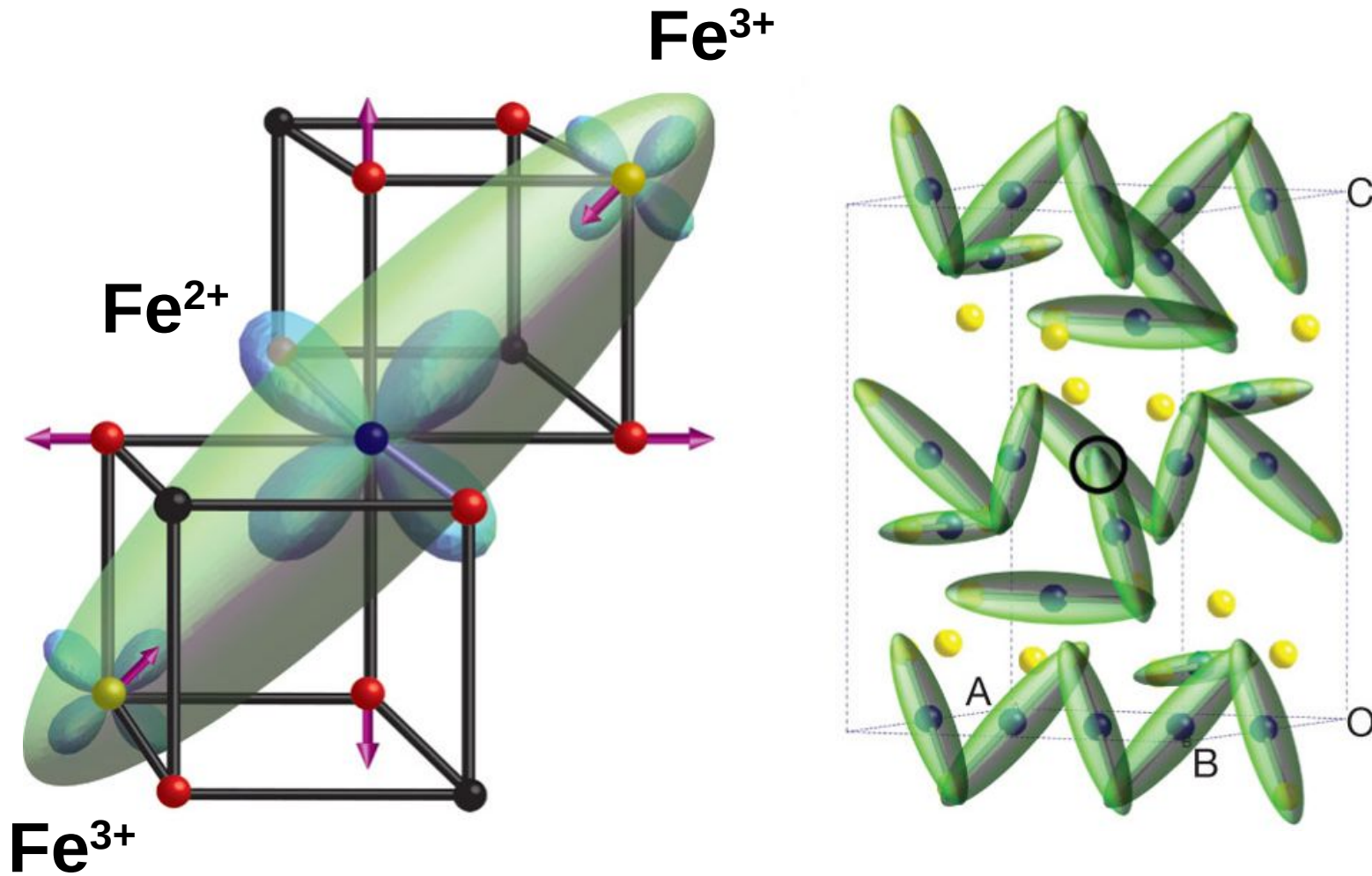


Cc $T < T_v = 125$ K



Fe(A)³⁺ - tetrahedral position
Fe(B)^{2.5+} - octahedral position
O - oxygen

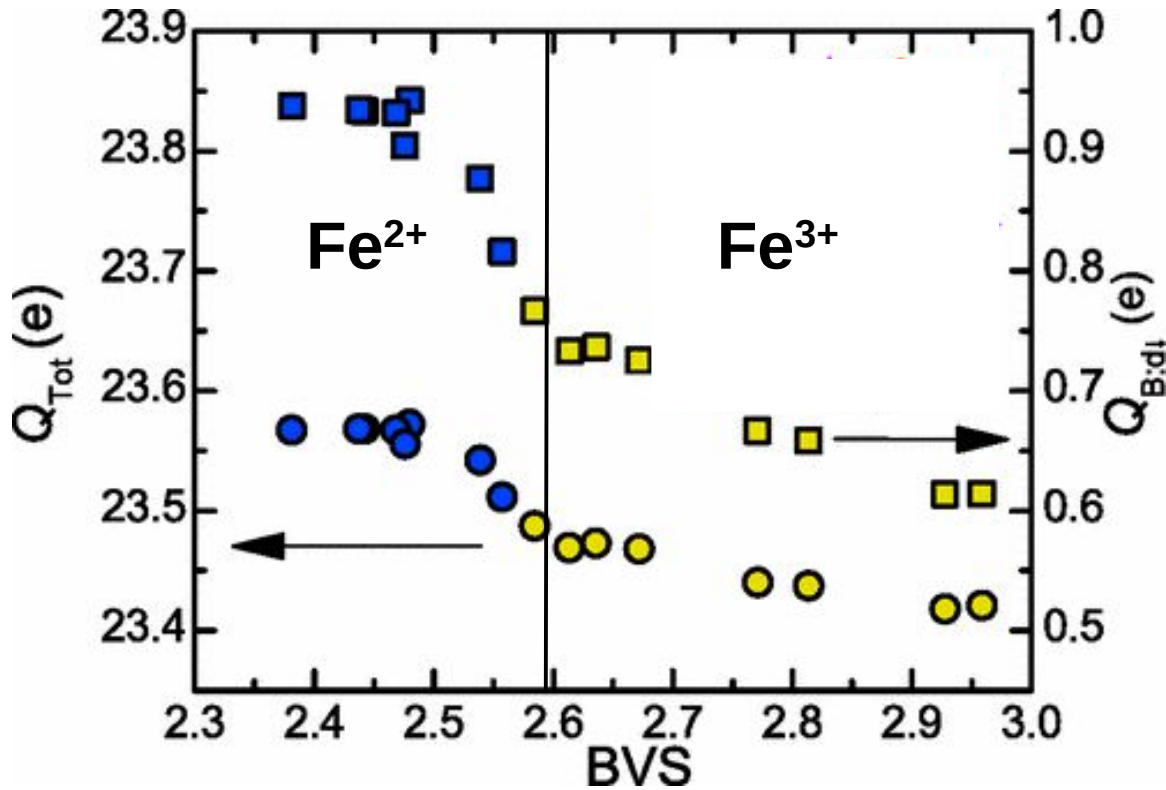
Trimerons



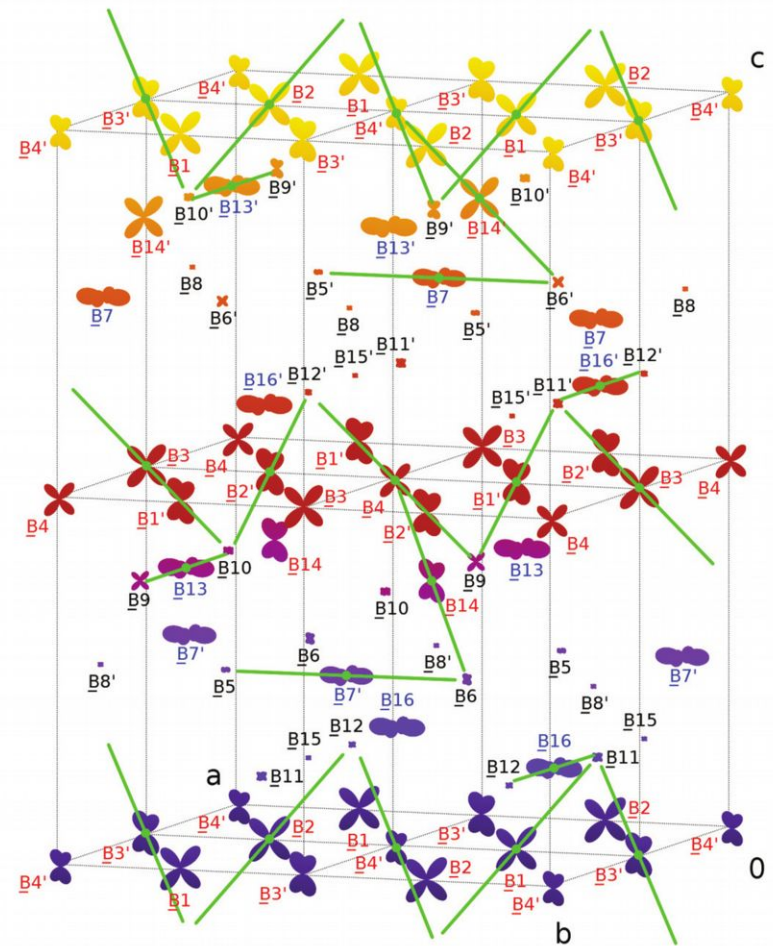
M. R. Senn, J. P. Wright, and J. P. Attfield, Nature 481, 173 (2012)

Charge-orbital order

Fe(B) – 16 different crystallographic sites (charges) in Cc



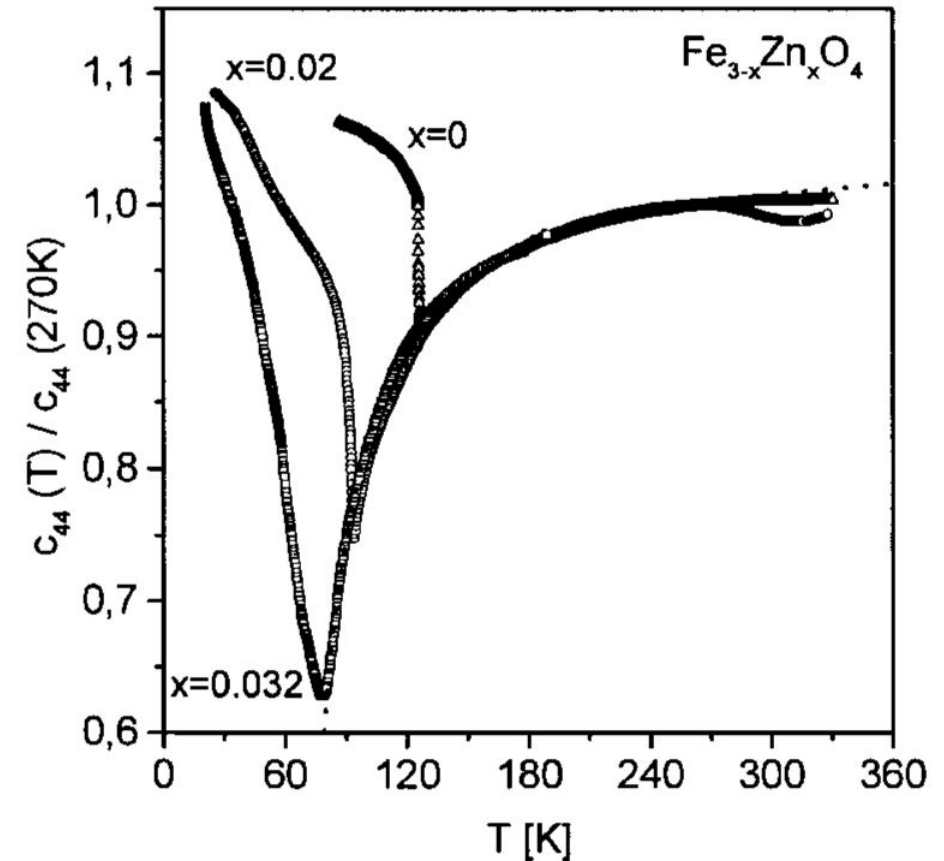
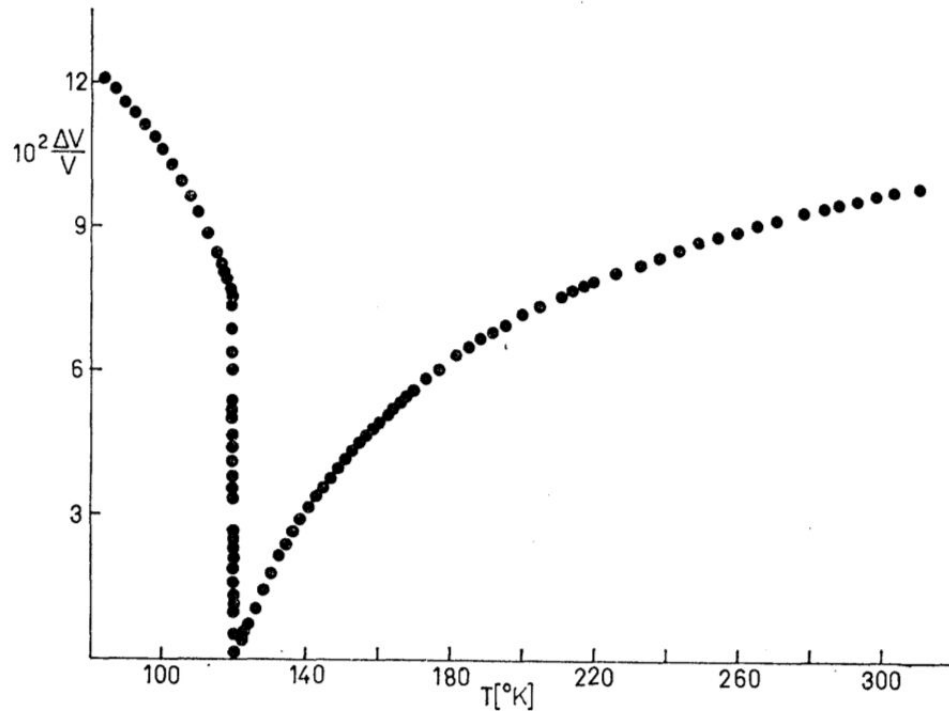
M. S. Senn et al., Phys. Rev. B 85, 125119 (2012)



R. Reznicek et al., Phys. Rev. B 91, 125134 (2015)

Critical softening of c_{44} above T_v

T. J. Moran and B. Luthi, Phys. Rev. 187, 710 (1969)



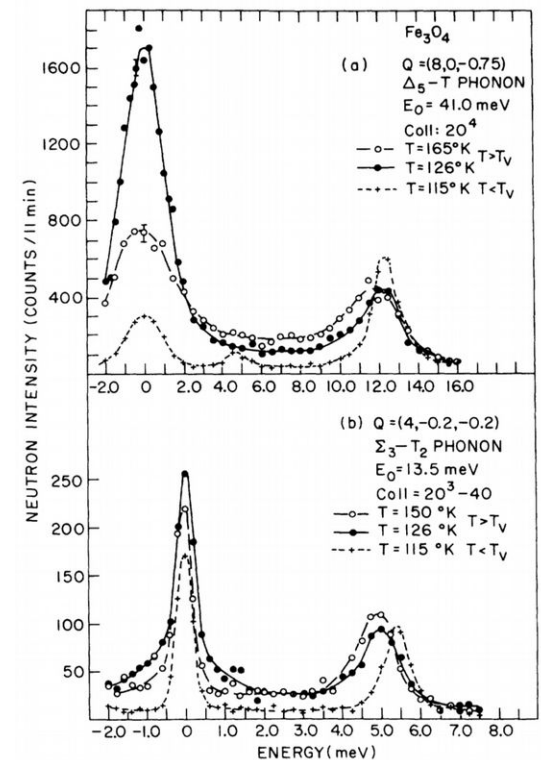
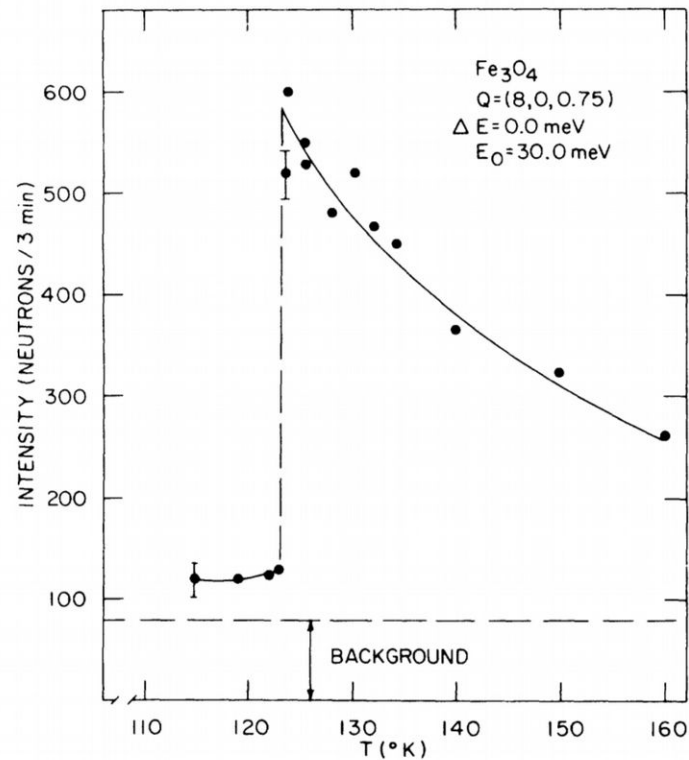
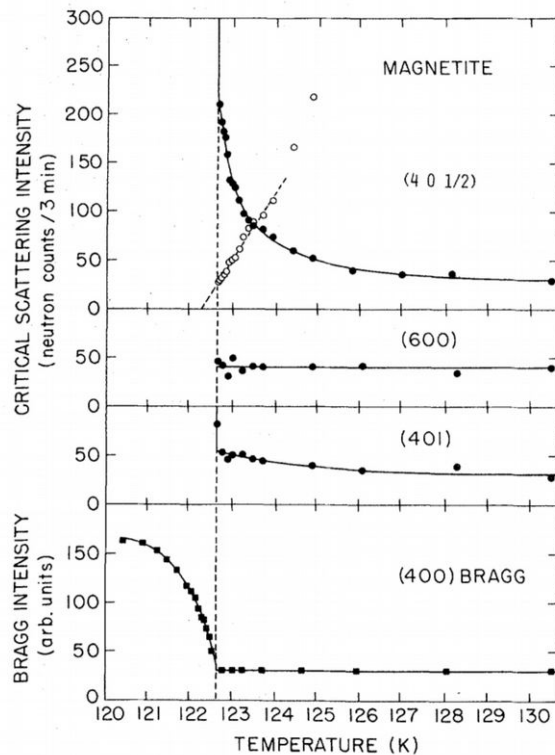
H. Schwenk, S. Bareiter, C. Hinkel, B. Luthi, Z. Kakol, A. Koslowski, and J. M. Honig, Eur. Phys. J. B 13, 491 (2000)

The critical behavior of elastic constant c_{44} was explained in terms of bilinear coupling of the elastic strain to a fluctuation mode of the charge ordering field of T_{2g} symmetry

Critical neutron scattering above T_V

Diffuse scattering at the same wave vectors as the superlattice reflections of the monoclinic phase

Diffuse scattering at incommensurate q vectors is observed in broad temperature range

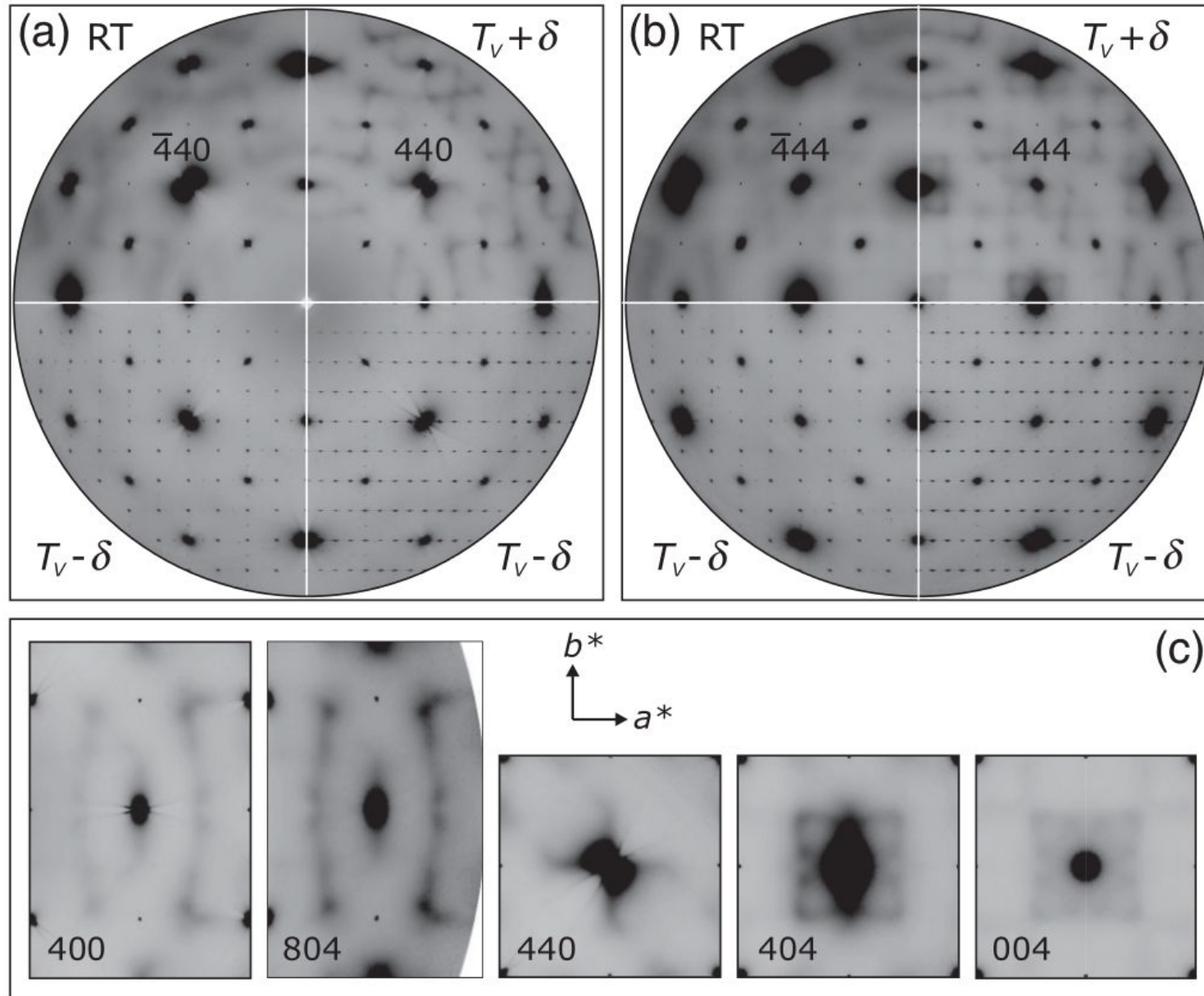


Y. Fujii, G. Shirane, and Y. Yamada,
Phys. Rev. B 11, 2036 (1975)

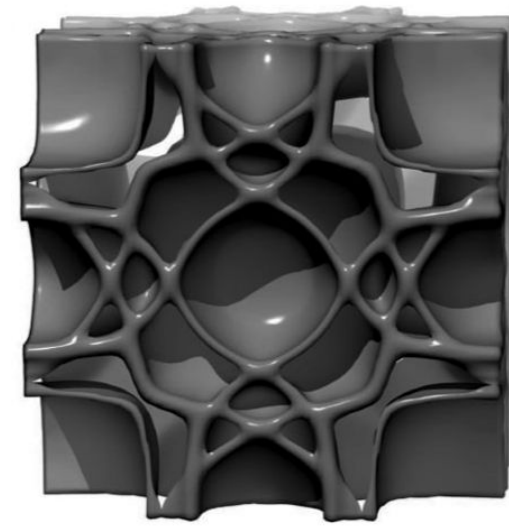
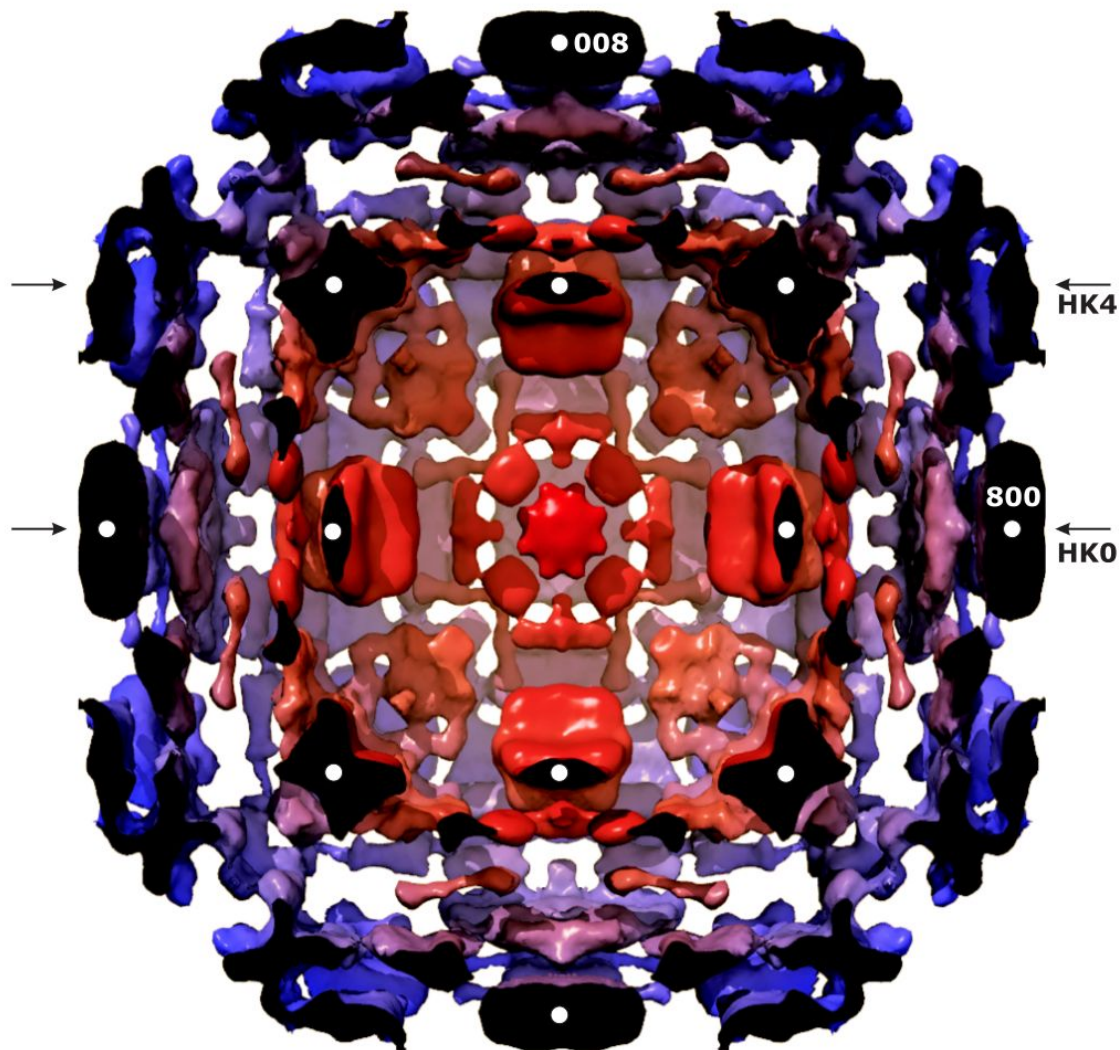
S. M. Shapiro, M. Iizumi, and G. Shirane,
Phys. Rev. B 14, 200 (1976)

Neutron diffuse scattering centered at zero energy (central peak) is coupled with transverse acoustic (TA) phonons

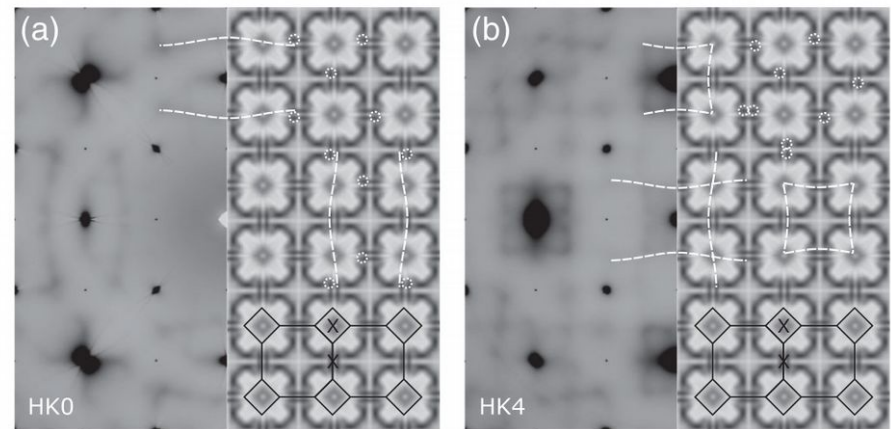
X-ray diffuse scattering (ID28, ESRF)



X-ray diffuse scattering (ID28, ESRF)



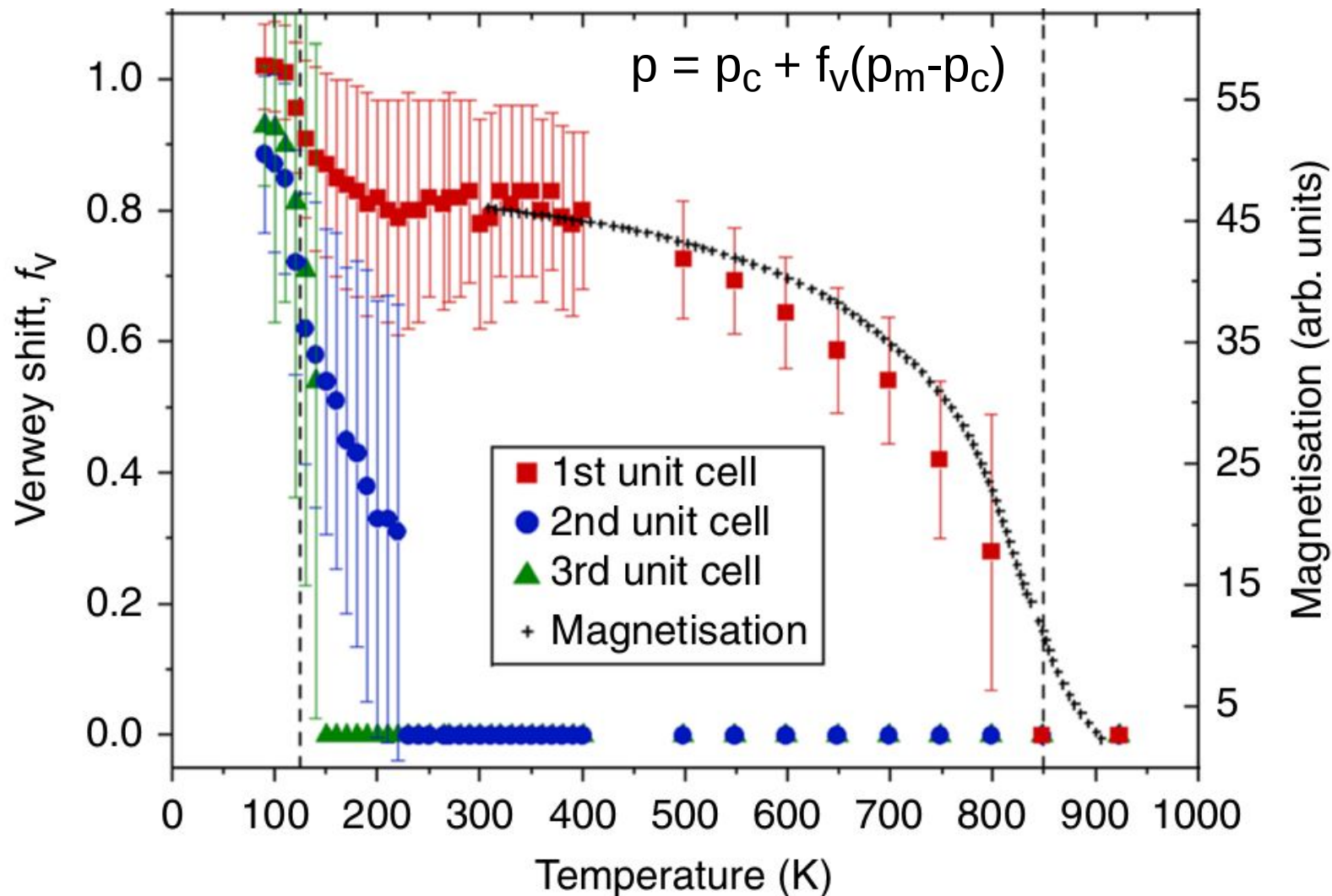
$$q = 2k_F$$



A. Bosak, D. Chernyshov, M. Hoesch, P. Piekarczyk, M. Le Tacon, M. Krisch, A. Kozłowski, A. M. Oleś, and K. Parlinski, Phys. Rev. X 4, 011040 (2014)

Short-range fluctuations up to T_c

The structural fluctuations responsible for the Verwey transition emerge with the long-range magnetic order below the Curie transition and scale with the magnetisation



G. Perversi, E. Pachoud, J. Cumby, J. M. Hudspeth, J. P. Wright, S. A.J. Kimber and J. P. Attfield, Nature Communications 10, 2857 (2019)

Lattice dynamics

K. Parlinski, Z. Q. Li, and Y. Kawazoe, Phys. Rev. Lett. 78, 4063 (1997)

- crystal structure optimization (DFT, VASP)

$$E_{\text{tot}} = \min \quad F_i(\mu) = 0$$

- Hellmanna-Feynman forces

$$F_i(\mu) = - dE_{\text{tot}}/du_i(\mu)$$

- force constants matrix (Phonon)

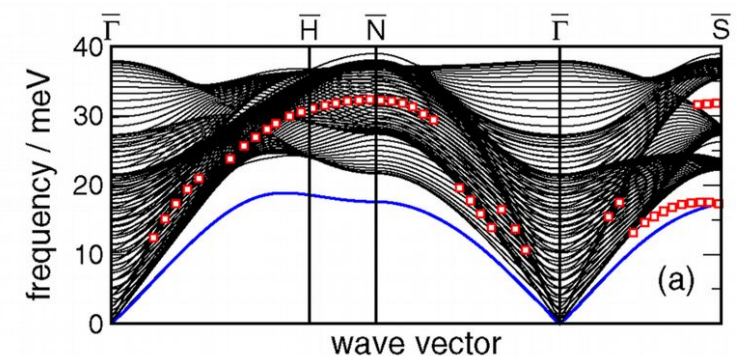
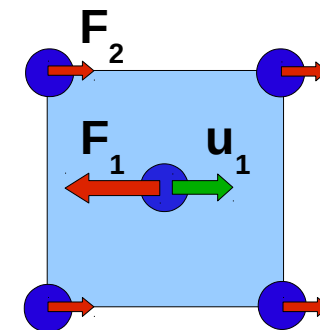
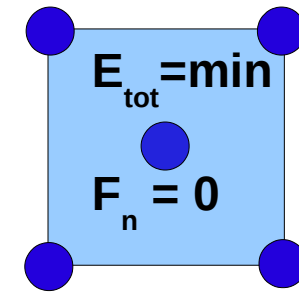
$$F_i(\mu) = - \sum \Phi_{ij}(\mu, \nu) u_j(\nu)$$

- dynamical matrix $\Phi(\mu, \nu) \Rightarrow D(k, \mu, \nu)$

- dispersion curves, polarisation vectors, DOS

$$D(k, \mu, \nu) e(k, j) = \omega^2(k, j) e(k, j)$$

Method has been applied to bulk crystals, surfaces, nanostructures, disordered systems



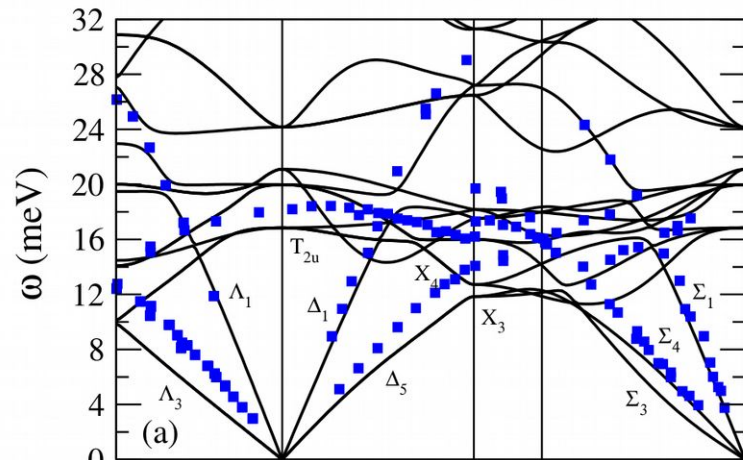
Phonon dispersions at Fe(110) surface

Phonons in magnetite

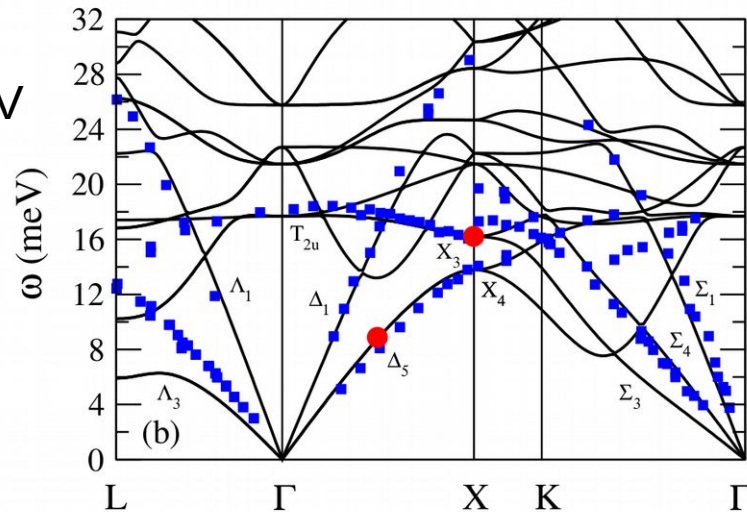
P. Piekarz, K. Parlinski, A. M. Oleś, Phys. Rev. Lett. 97, 156402 (2006),
 Phys. Rev. B 76, 165124 (2007)

DFT, VASP, LDA+U, $U = 4$ eV, $J = 0.8$ eV

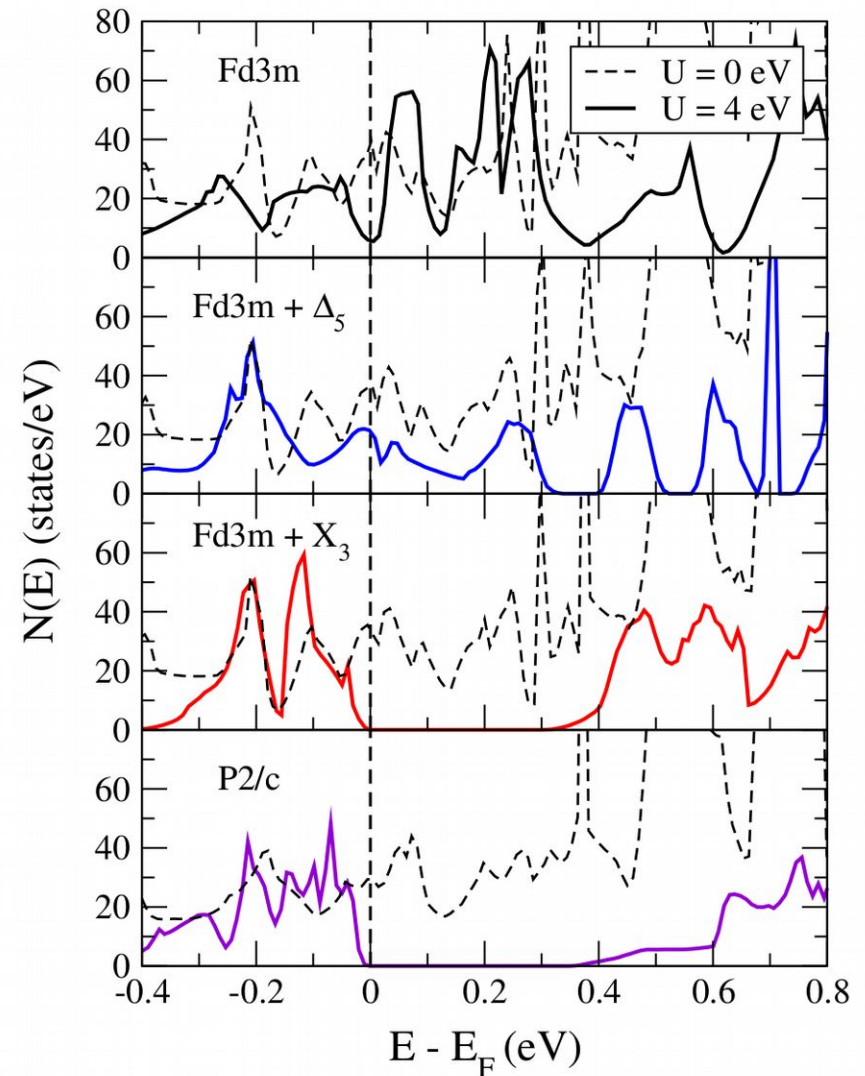
$U = 0$



$U = 4$ eV

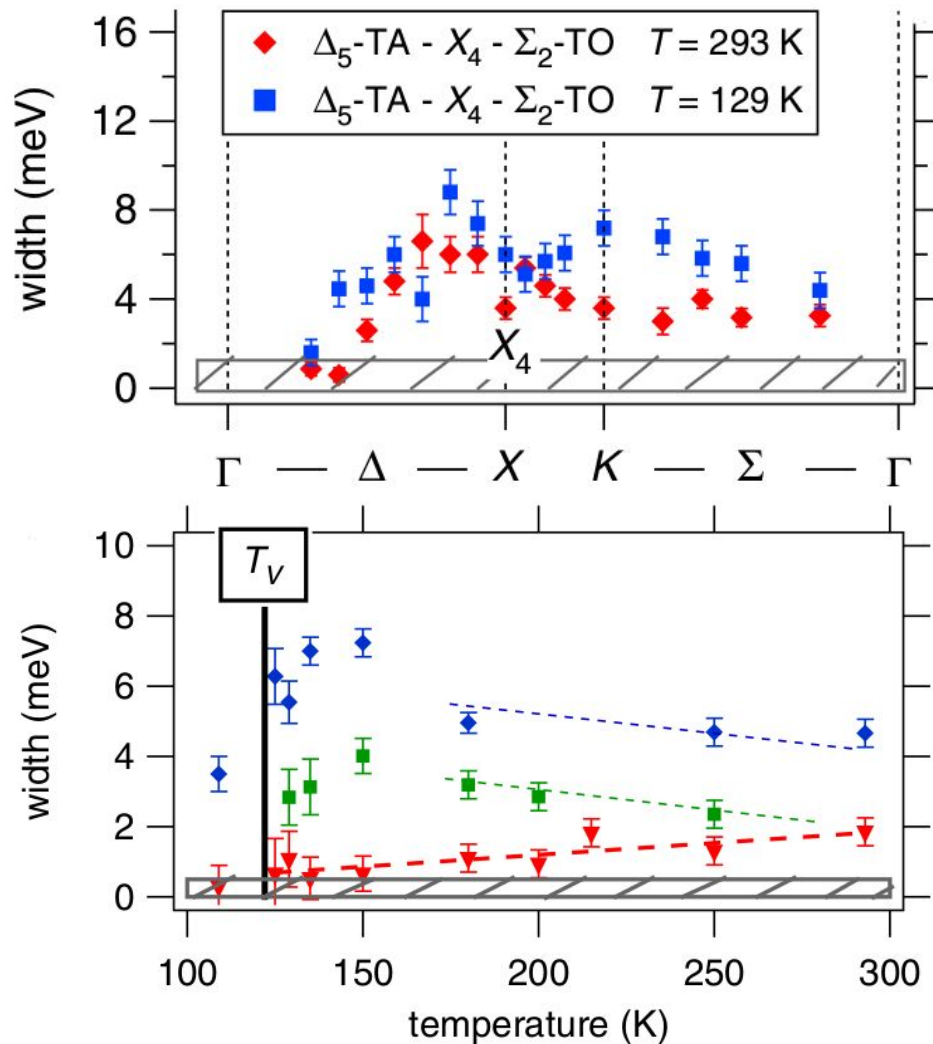


Fd-3m \rightarrow X₃ + Δ_5 \rightarrow P2/c

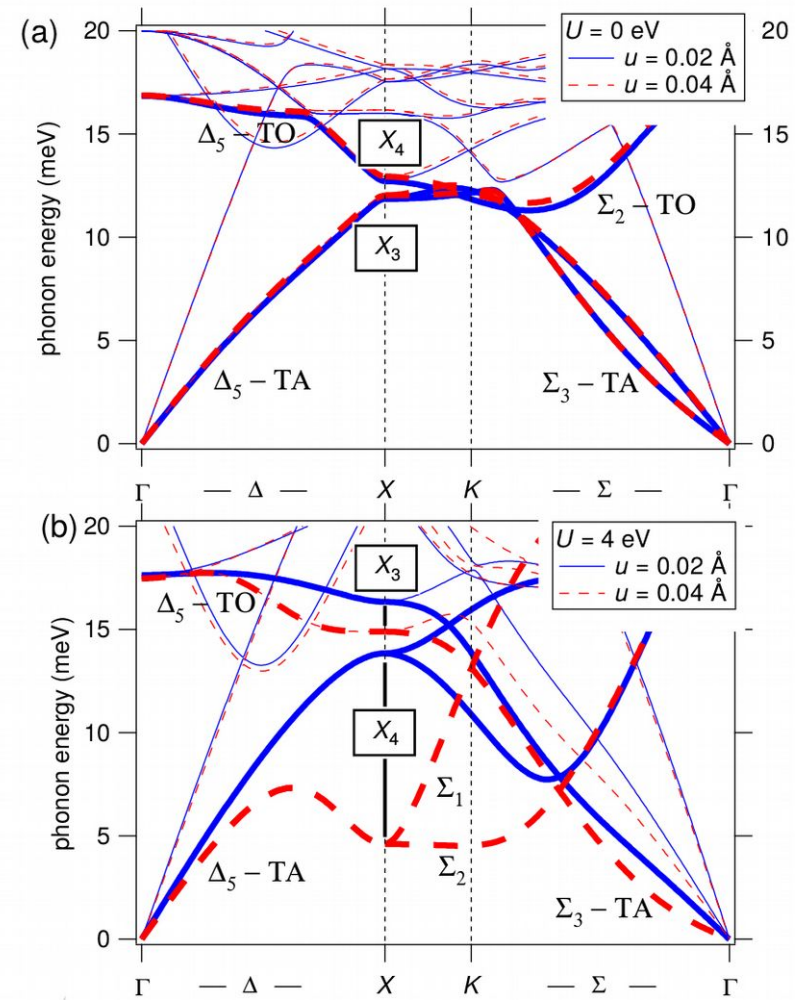


INS E. J. Samuelsen and O. Steinsvoll,
 Phys. Status Solidi B 61, 615 (1974)

Inelastic X-ray scattering (ID28, ESRF)



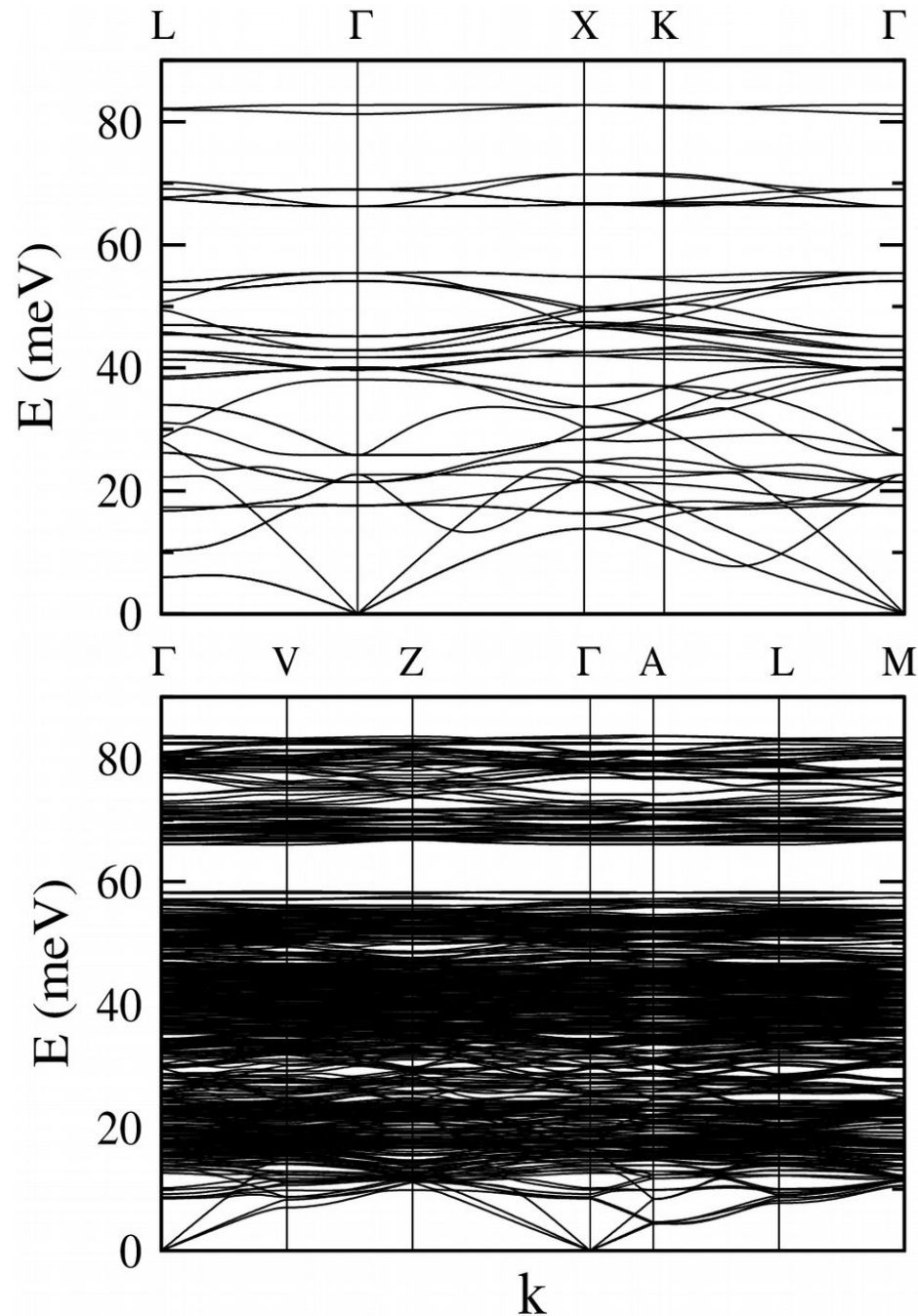
anomalous phonon broadening



strong anharmonicity induced by electron-phonon coupling

M. Hoesch, P. Piekarczyk, A. Bosak, M. Le Tacon, M. Krisch, A. Kozłowski, A. M. Oleś, K. Parlinski, Phys. Rev. Lett. 110, 207204 (2013)

Dispersion relations in Cc structure



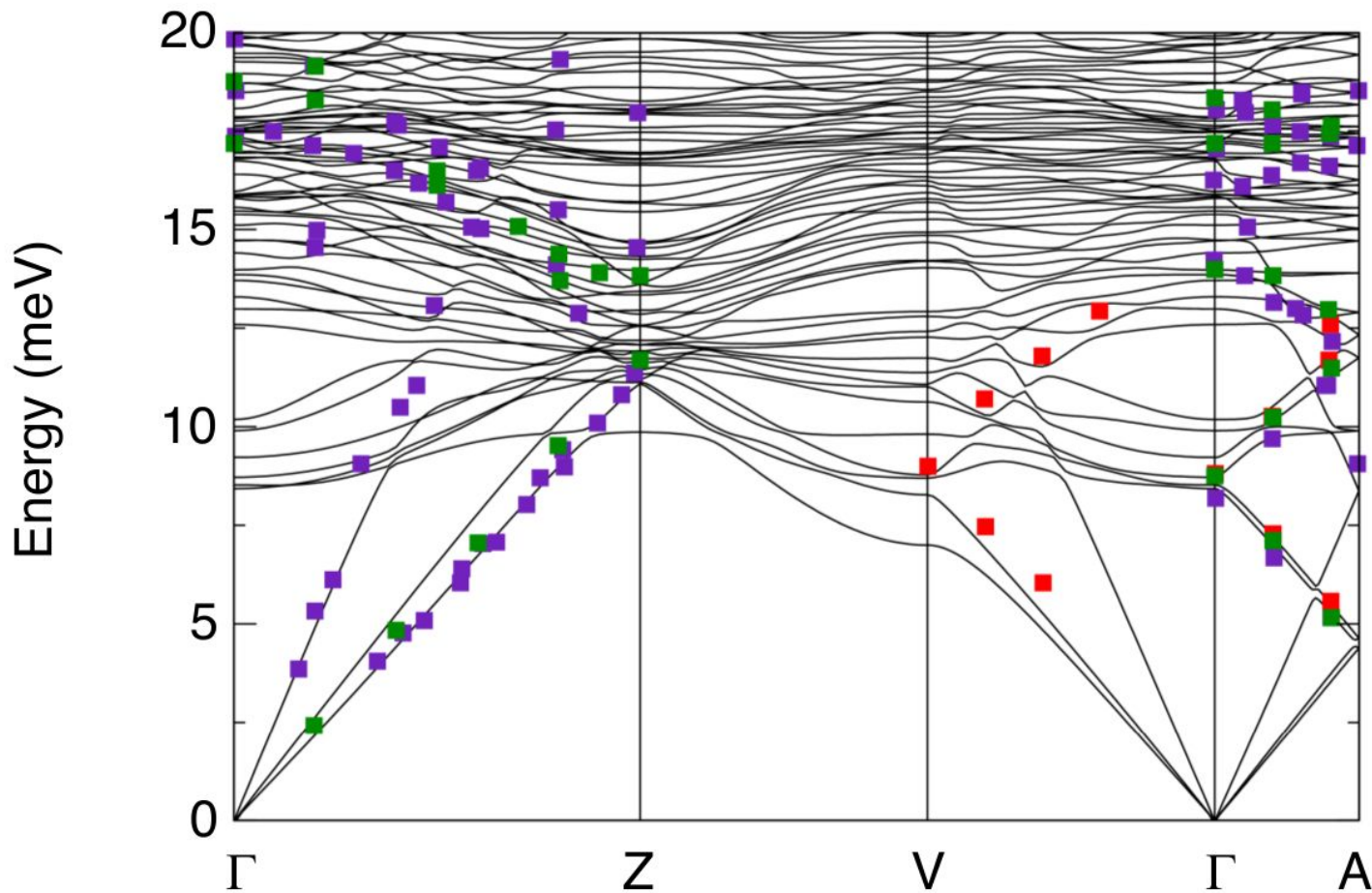
Fd-3m

56 atoms in supercell
14 atoms in primitive cell
42 phonon dispersions

Cc

224 atoms in supercell
112 atoms in primitive cell
336 phonon dispersions

Dispersion relations in Cc structure

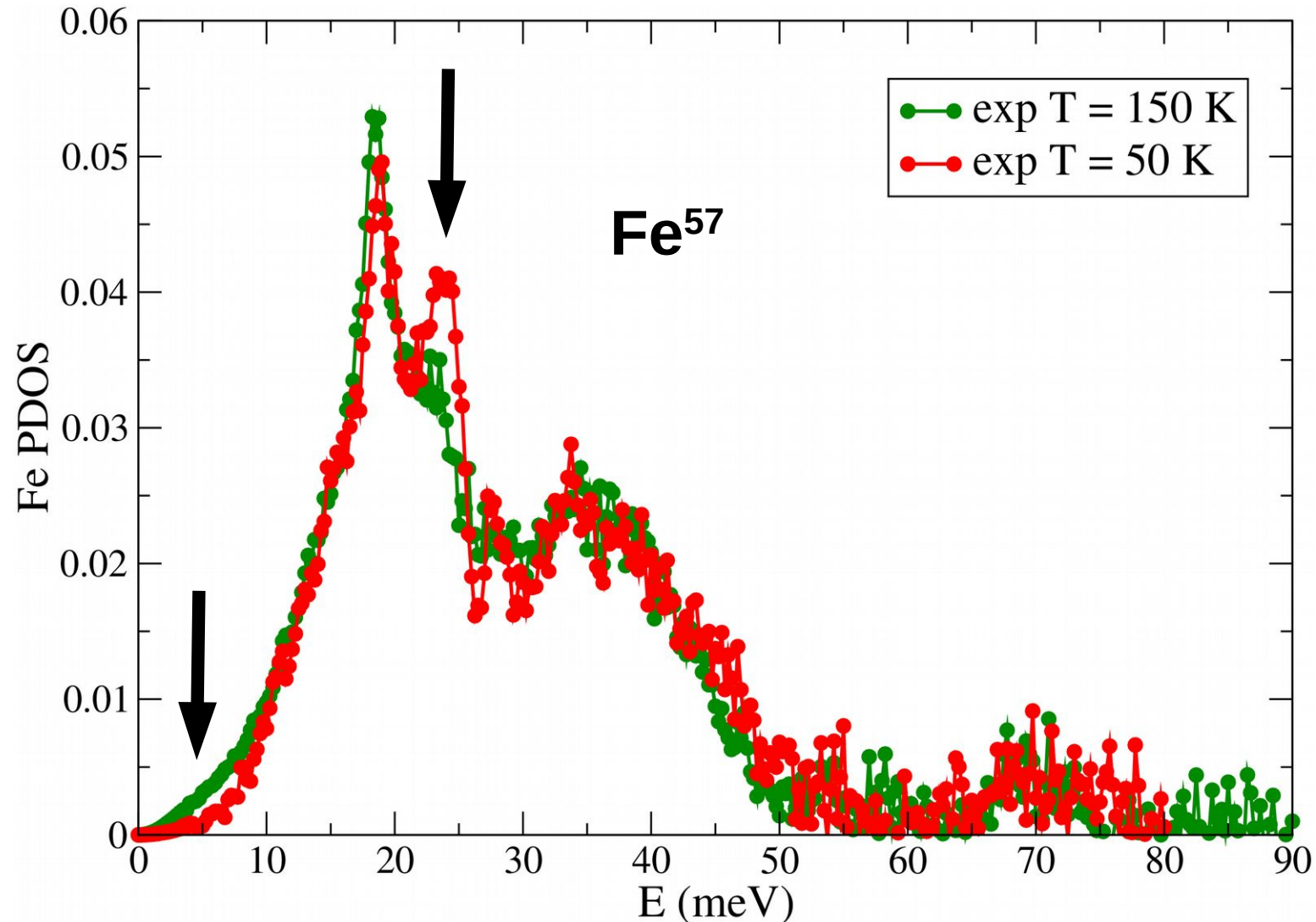


INS $T > T_V$ (violet) E. J. Samuelsen and O. Steinsvoll, Phys. Status Solidi B 61, 615 (1974)

INS $T < T_V$ (red) S. Borroni, et al., New J. Phys. 19, 103013 (2017)

IXS $T > T_V$ (green) M. Hoesch, et al., Phys. Rev. Lett. 110, 207204 (2013)

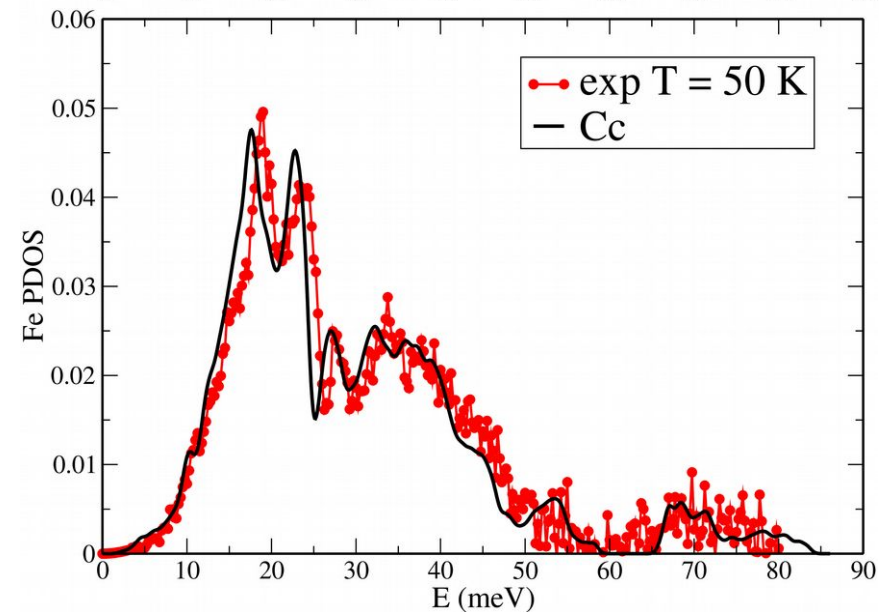
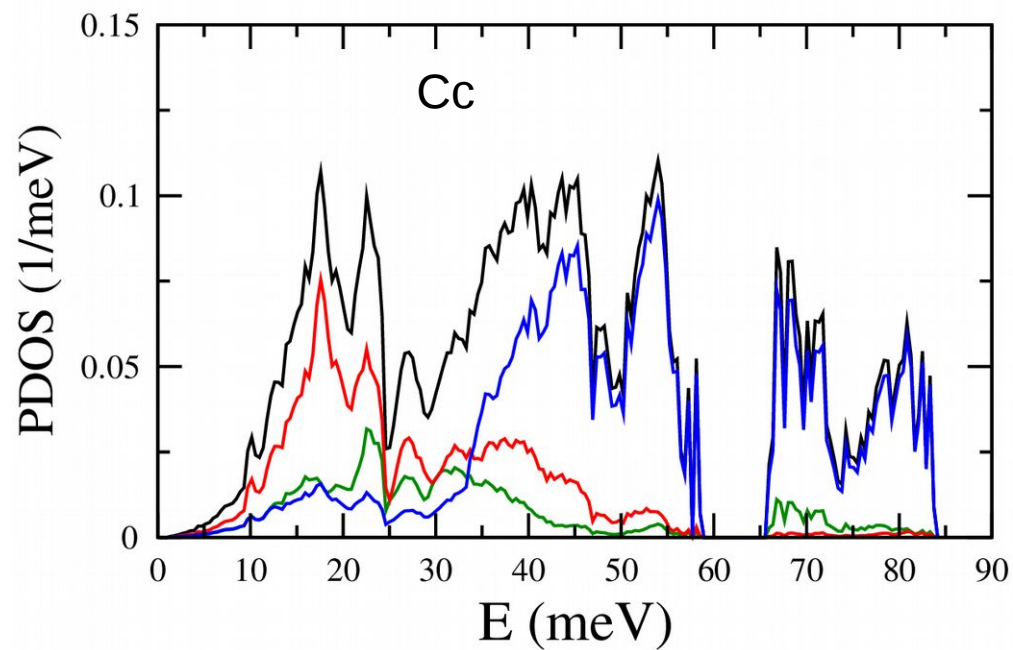
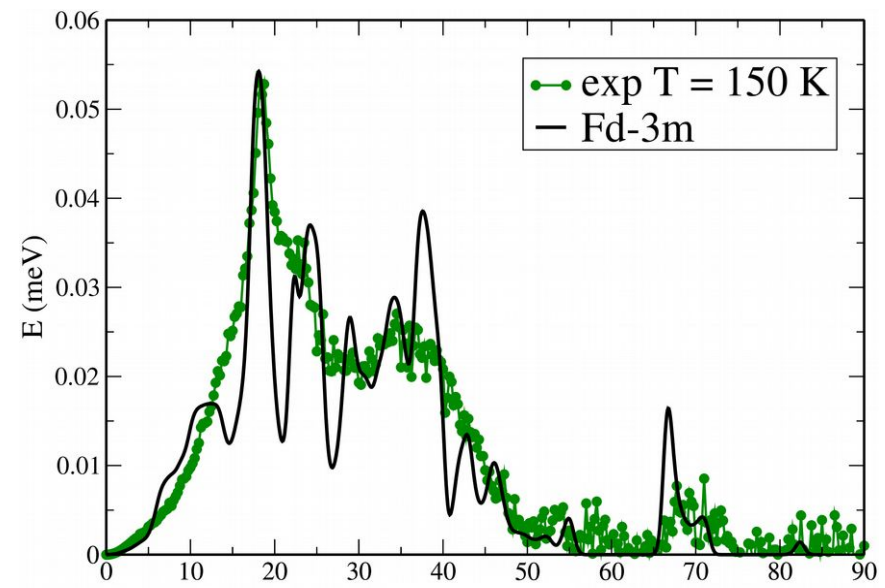
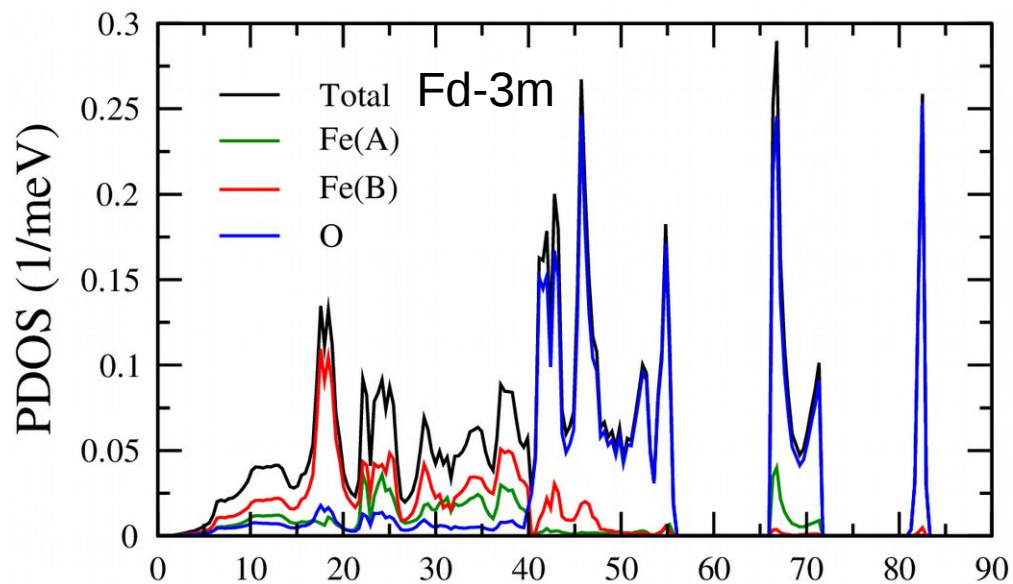
Nuclear inelastic scattering (ID18, ESRF)



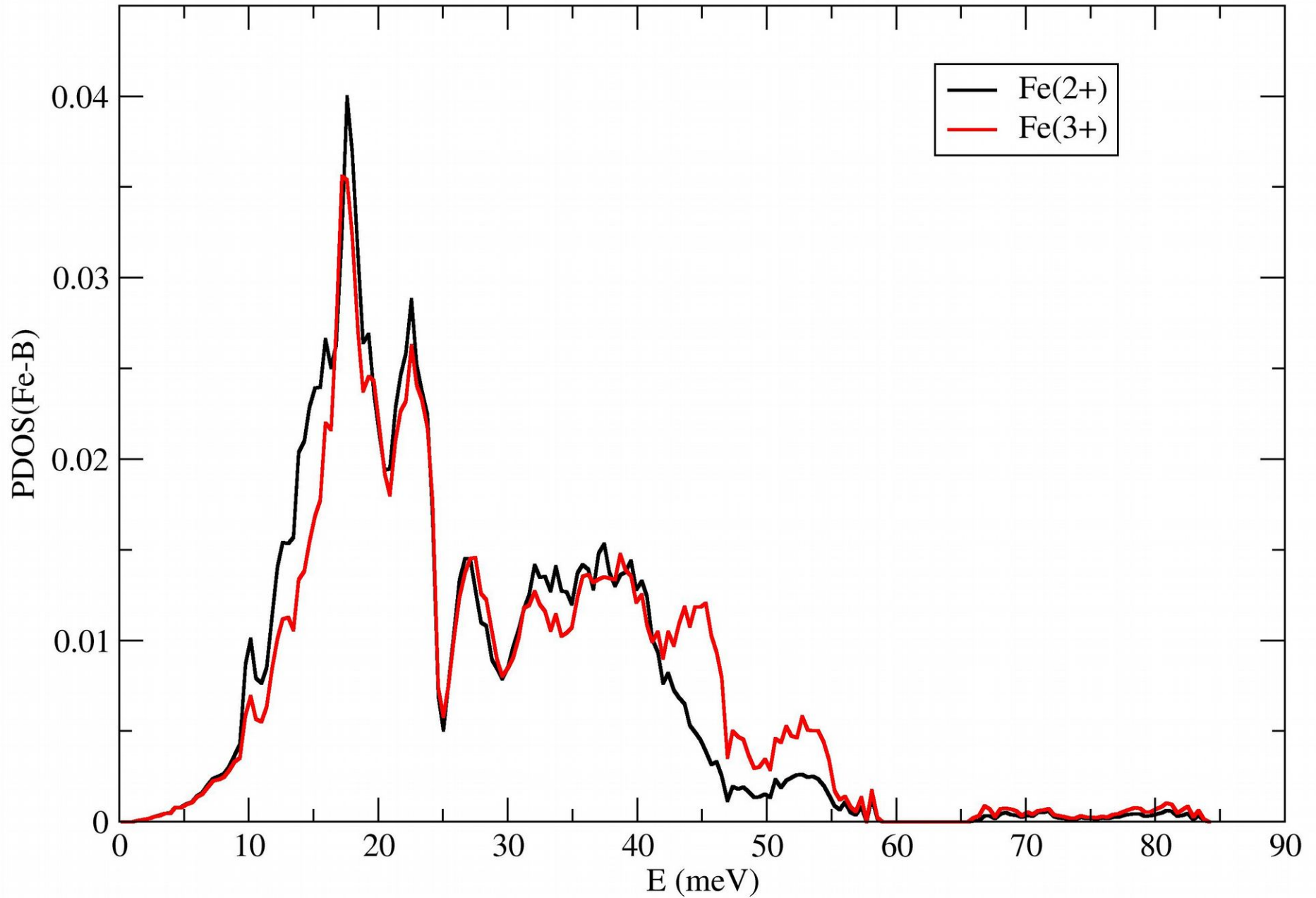
B. Handke, A. Kozłowski, K. Parlinski, J. Przewoźnik, T. Ślęzak, A. I. Chumakov, L. Niesen, Z. Kąkol, and J. Korecki, Phys. Rev. B 71, 144301 (2005)

T. Kołodziej, A. Kozłowski, P. Piekarczyk, W. Tabiś, Z. Kąkol, M. Zając, Z. Tarnawski, J. M. Honig, A. M. Oleś, K. Parlinski, Phys. Rev. B 85, 104301 (2012)

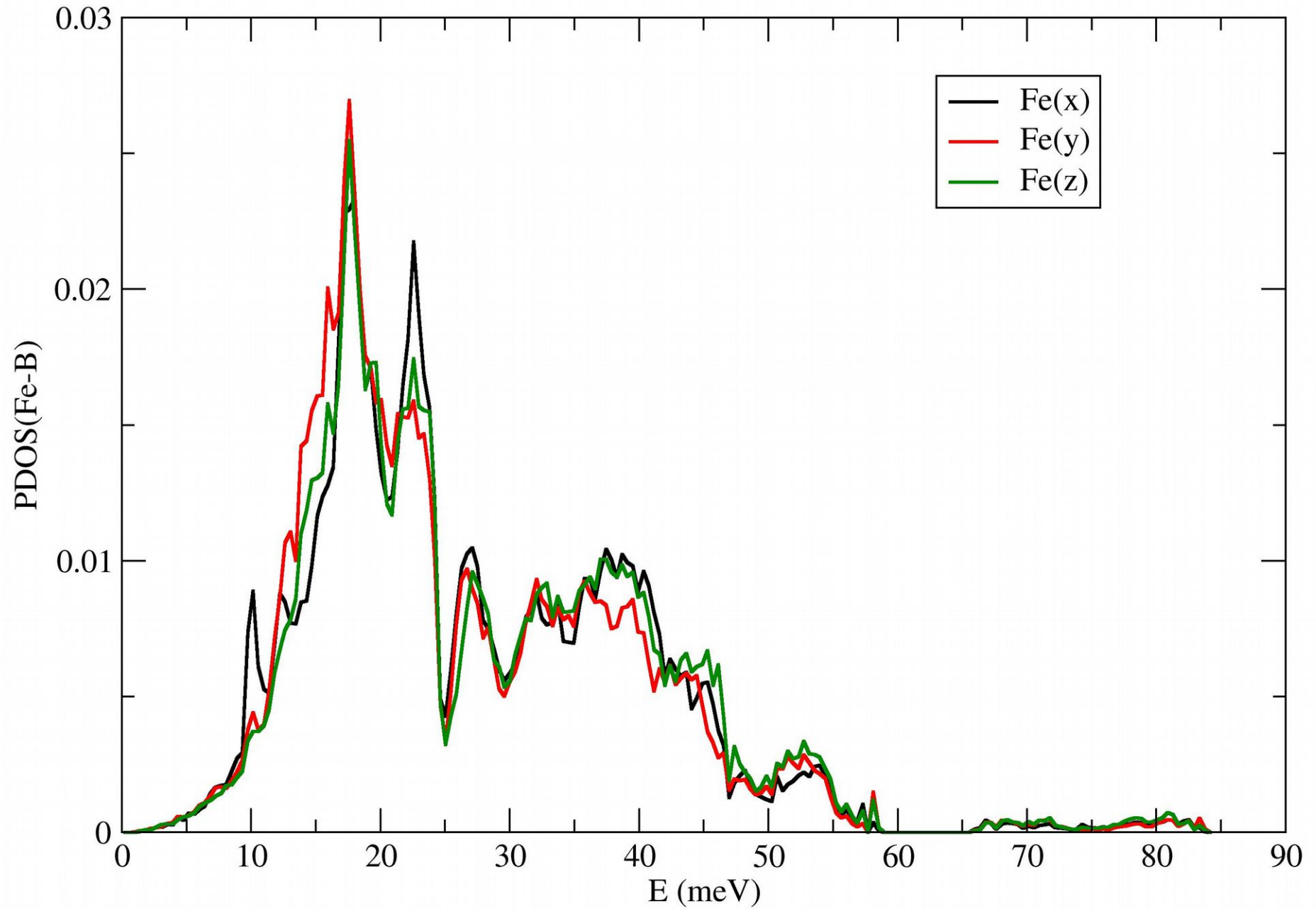
Phonon Fe DOS Fd-3m vs Cc



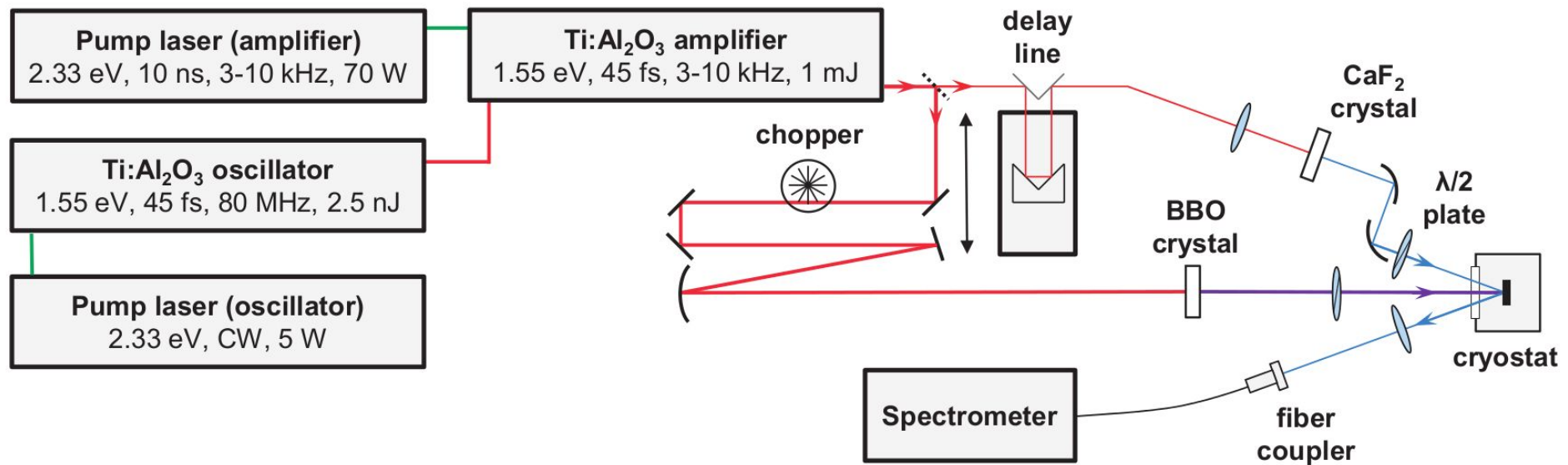
Phonon Fe DOS Cc Fe2+ vs Fe3+



Phonon Fe DOS Cc x, y, z



Pump-probe experiment (EPFL)



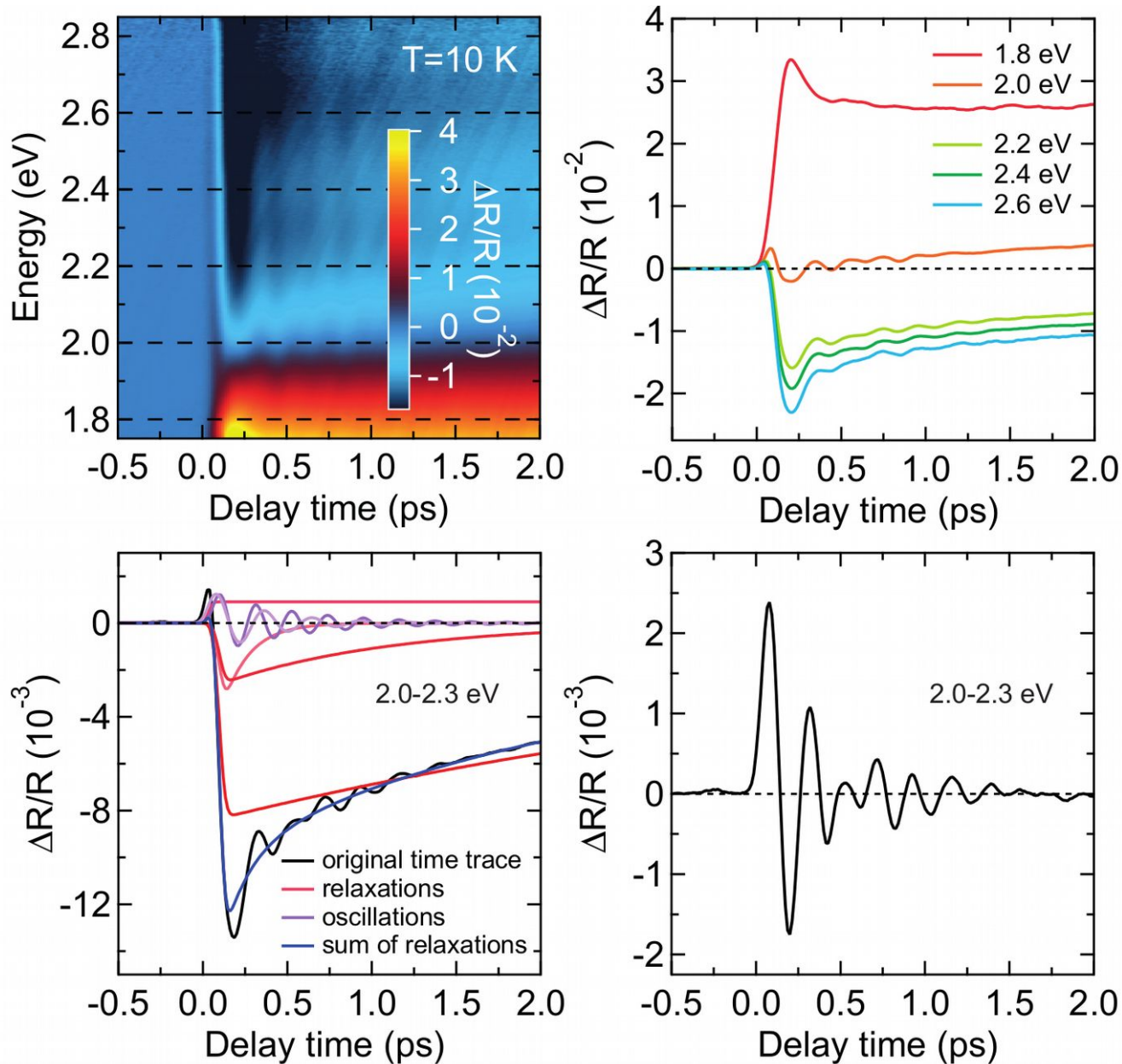
The pump-probe ultrafast spectroscopy scheme.

A sequence of laser pulses, the pump pulses, is sent to the sample. To measure the consequent response, delayed replica of the pump pulses, the probe pulses, are also sent to the sample, in a small spot wherein the intensity of the pump pulses is homogeneous. The repetition rate and the fluence, i.e. the energy per unit area, of the pump pulses are chosen so that the sample returns to equilibrium between consecutive pump pulses. Therefore, for a given time delay between pump and probe pulses, all probe pulses measure an identical state of the sample. After enough statistics on the probe pulses is collected, the time delay between pump and probe pulses is changed, to progressively construct a sequence of data points, representative of the dynamics upon impulsive photoexcitation.

Simone Borroni, Ph.D. Thesis, "New Insights into the Verwey Transition in Magnetite" (2018)

Pump-probe experiment (EPFL)

Differential reflectivity as a function of pump-probe delay time and probe photon energy



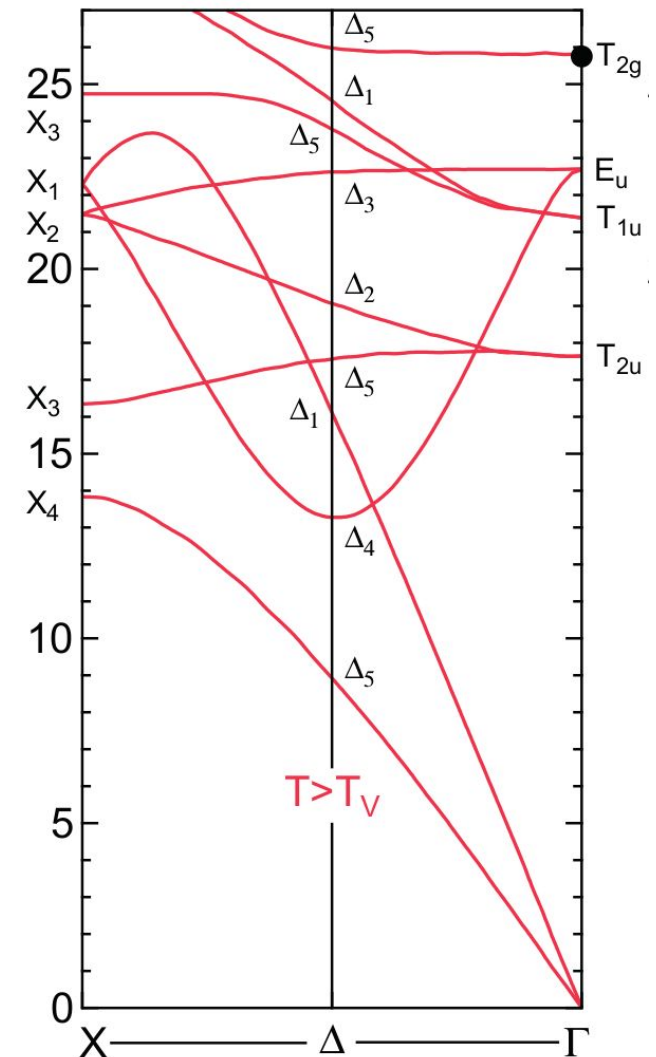
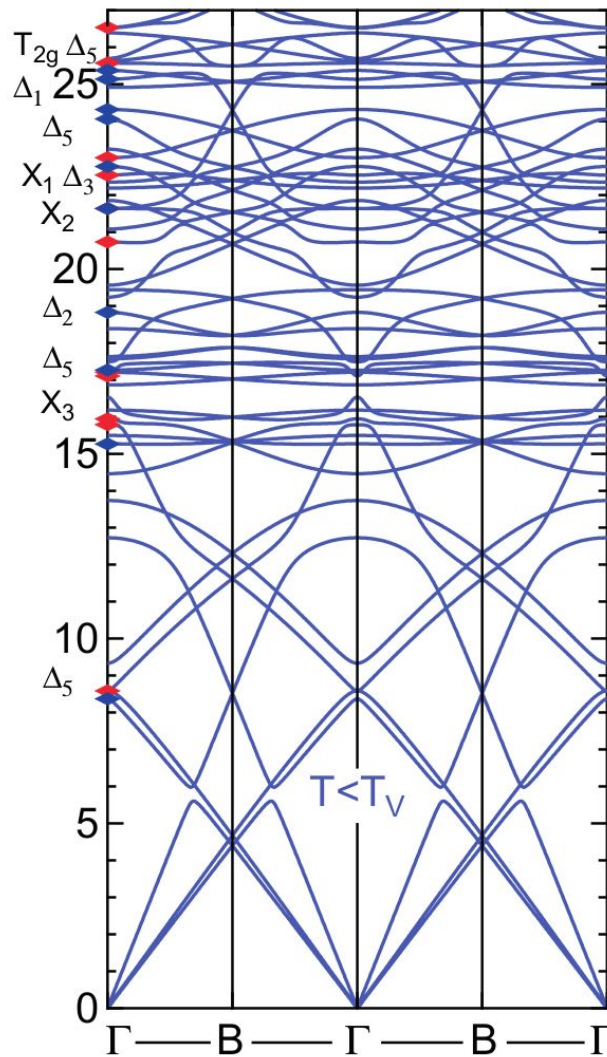
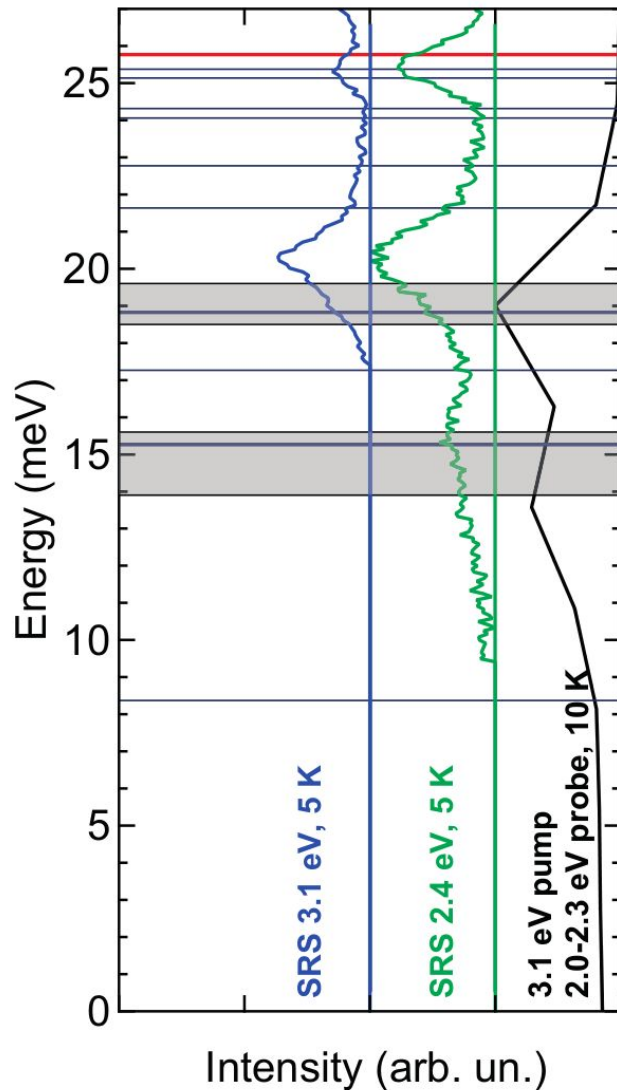
Raman modes

Spontaneous Raman spectra (SRS)
and coherent pump-probe response

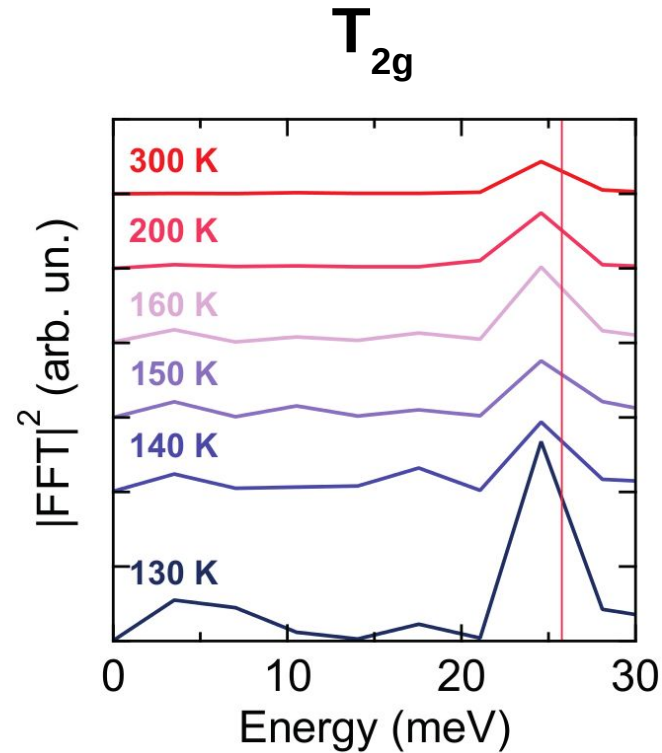
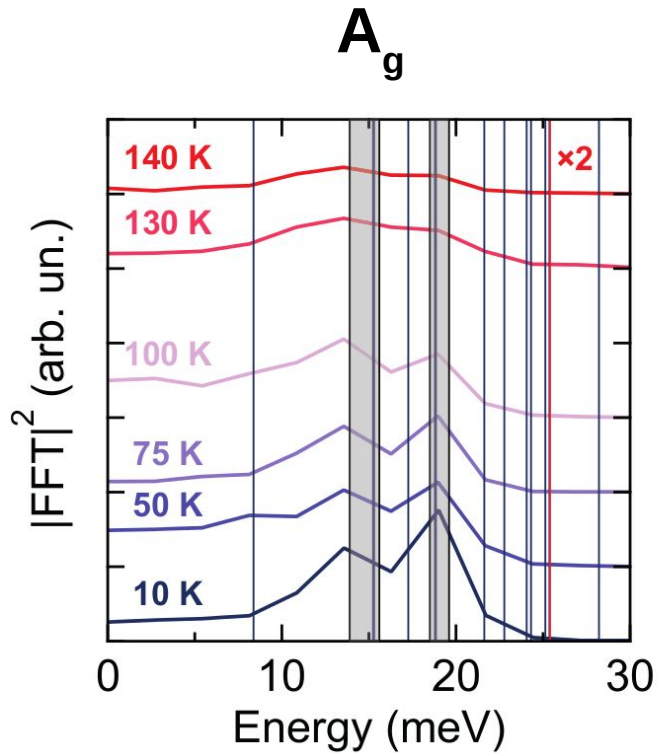
Ab initio DFT calculations

P2/c

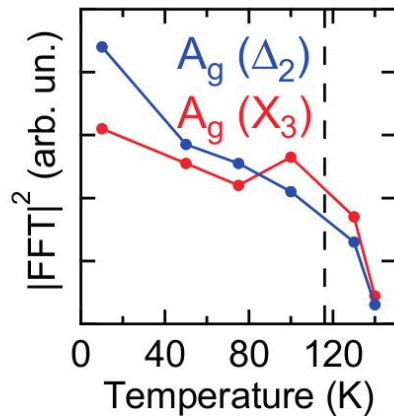
Fd-3m



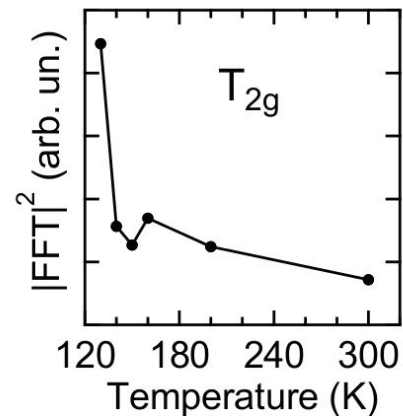
Raman modes



Forbidden A_g modes in cubic phase are observed above the Verwey temperature



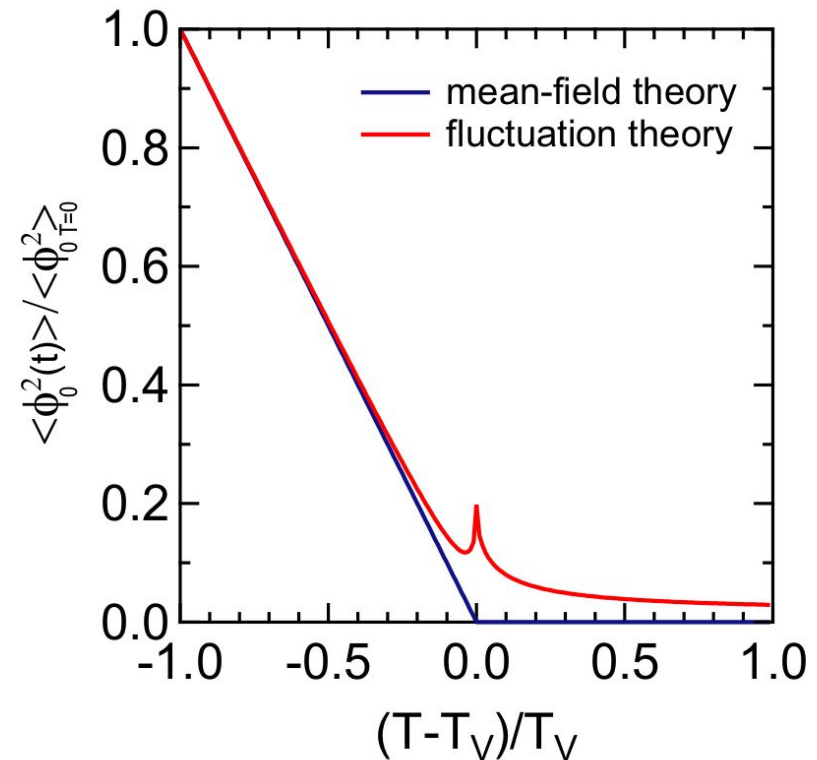
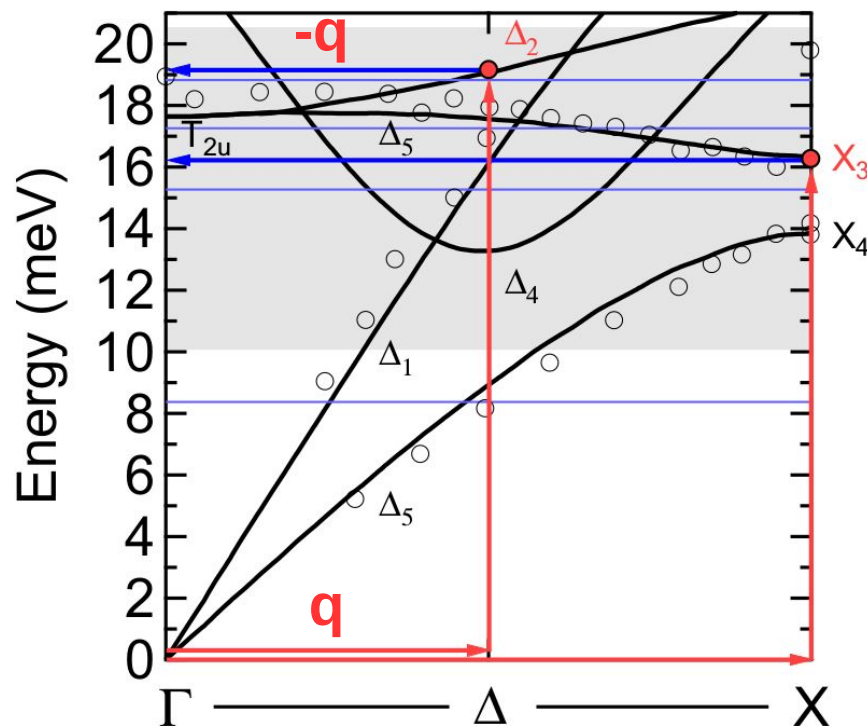
T_{2g} mode allowed in cubic phase



Raman modes

A second-order Raman process takes place, in which an electronic mode of wave vector q is excited together with a phonon mode of wave vector $-q$, so that the total wave vector is conserved

The coupling between lattice vibrations at finite momentum and fluctuations of the electronic ordering field above the Verwey transition in magnetite

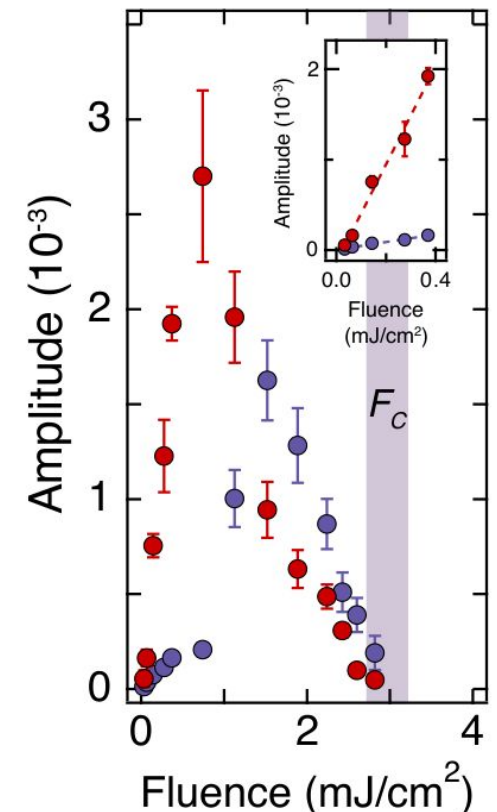
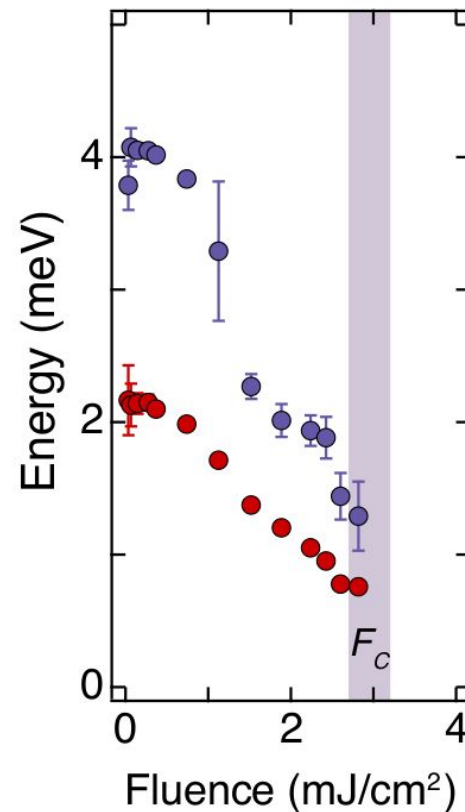
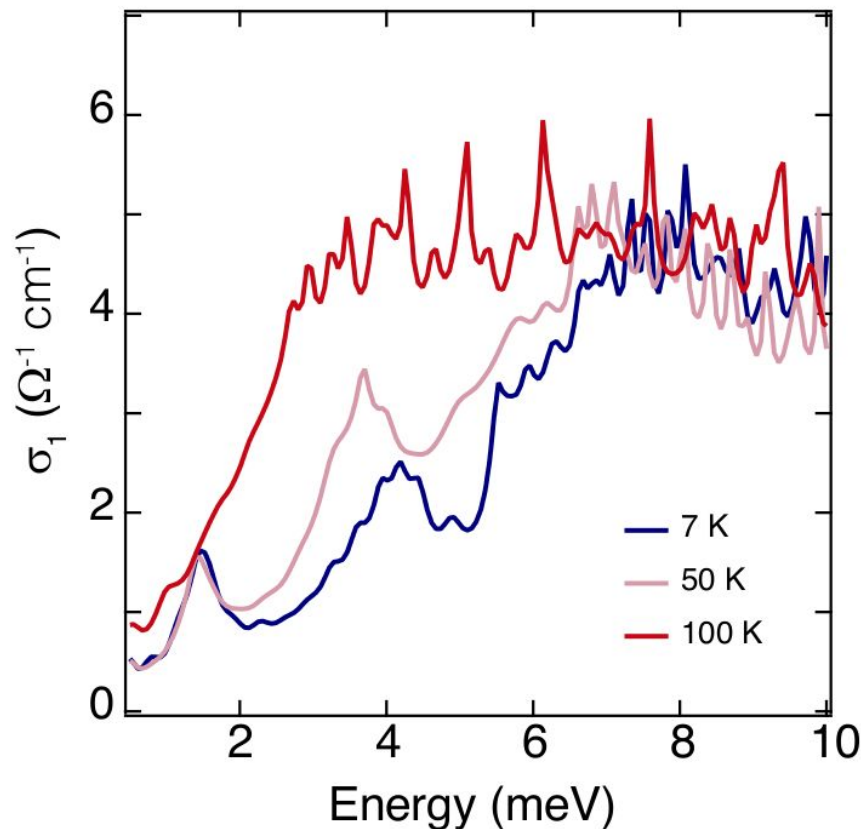


S. Borroni, E. Baldini, V. M. Katukuri, A. Mann, K. Parlinski, D. Legut, C. Arrell, F. van Mourik, J. Teyssier, A. Kozłowski, P. Piekarczyk, O. V. Yazyev, A. M. Oleś, J. Lorenzana, and F. Carbone, Phys. Rev. B 96, 104308 (2017)

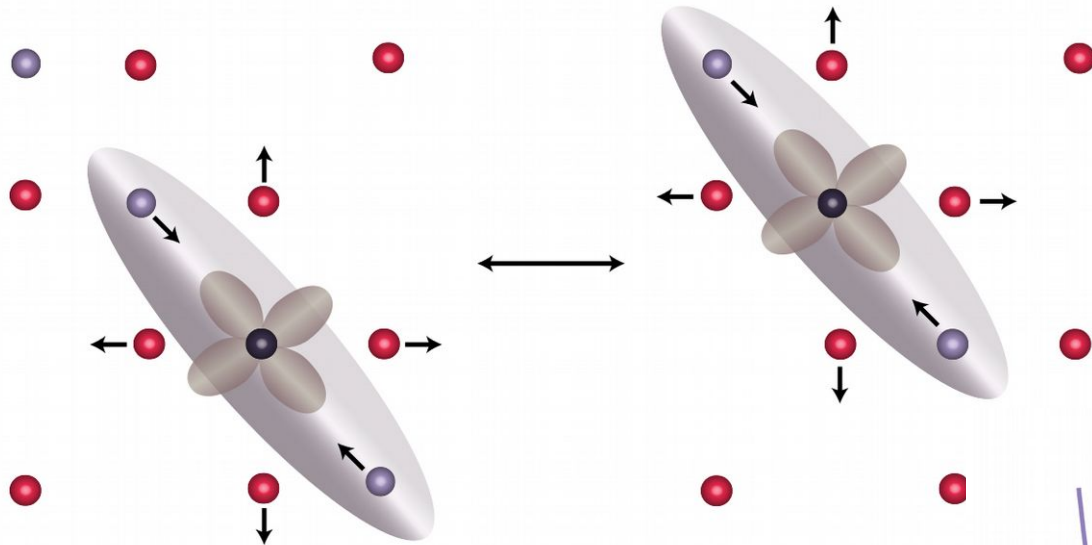
Low-energy charge fluctuations (MIT)

Spectroscopic signatures of the low-energy electronic excitations of the charge-orbital order (trimeron network) using terahertz light. By driving these modes coherently with an ultrashort laser pulse, we reveal their critical softening and hence demonstrate their direct involvement in the Verwey transition

These findings represent the first observation of soft modes in magnetite and shed new light on the cooperative mechanism at the origin of its exotic ground state

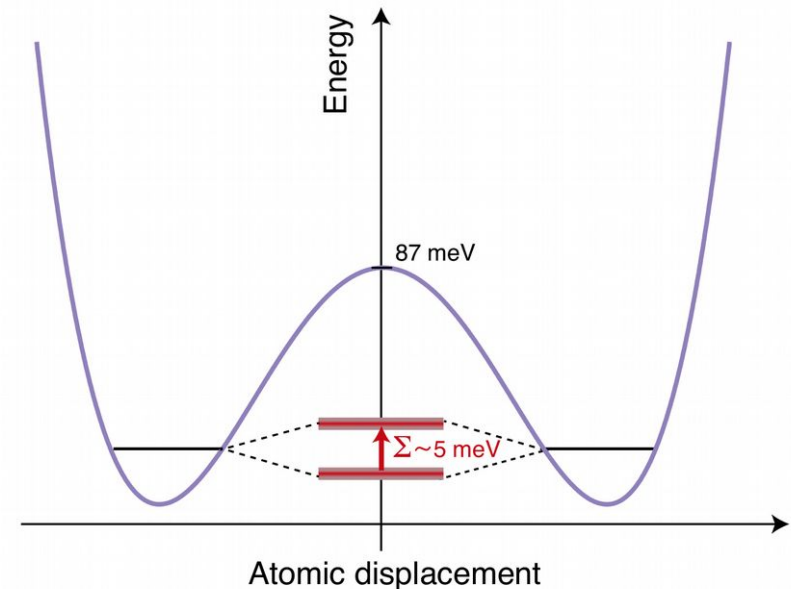


Low-energy charge fluctuations (MIT)



$$\Sigma = 2t = 2t_0 e^{-E_p/E_{ph}} \sim 5 \text{ meV}$$

$$t_0 = 0.2 \text{ eV}, E_p = 87 \text{ meV}, E_{ph} \sim 20 \text{ meV}$$



E. Baldini, C. A. Belvin, M. Rodriguez-Vega, I. O. Ozel, D. Legut, A. Kozłowski, A. M. Oleś, K. Parlinski, P. Piekarczyk, J. Lorenzana, G. A. Fiete, and N. Gedik, accepted in Nature Physics arXiv:2001.07815v1

Conclusions

- DFT studies revealed strong electron-phonon coupling, which opens the gap and induces monoclinic distortion
- Inelastic X-ray scattering found anomalous phonon broadening above T_v indicating anharmonic behaviour due to electron-phonon coupling
- X-ray diffuse scattering revealed new features at incommensurate q-points and short-range order in a wide range of temperatures
- Calculated phonon dispersion curves and phonon density of states for the Cc structure show very good agreement with the experimental data
- Forbidden phonon modes (below 25 meV) can be induced above T_v due to coupling with the critical fluctuations of the charge order
- New low-energy modes showing critical softening below T_v were discovered by optical conductivity and “pump-probe” experiments

This work was partially supported by NCN project 2017/25/B/ST3/02586